Survey of Active Acoustic Monitoring (AAM) Technologies

Volume V: Active Sonar Performance Factors

B. Maranda, L. Gilroy; J. Theriault; E. MacNeil
Defence R&D Canada Atlantic

Prepared For:
International Association of Oil & Gas Producers (OGP)
209-215 Blackfriars Road
London SEI 8NL, UK

This publication is protected by copyright. Any publication, use or release of this document is strictly prohibited without the expressed permission of Defence R&D Canada and International Association of Oil & Gas Producers (OGP).

Defence R&D Canada warrants that the work was performed in a professional manner conforming to generally accepted practices for scientific research and development.

This report is not a statement of endorsement by the Department of National Defence or the Government of Canada.

Defence R&D Canada – Atlantic

External Client Report
DRDC Atlantic ECR 2010-044
March 2010

Principal Author

B. Maranda

Principal Author

Approved by

D. Hutt

Section Head

Approved for release by

C. Hyatt

DRP Chair

This report has been completed for International Association of Oil and Gas Producers (OGP) under contract JIP22 08-06.

© Her Majesty the Queen in Right of Canada, as represented by the Minister of National Defence, 2010

© Sa Majesté la Reine (en droit du Canada), telle que représentée par le ministre de la Défense nationale, 2010

Abstract

Under the Exploration and Production (E&P) Sound and Marine Life Programme, a research study was carried out on the feasibility of the Active Acoustic Monitoring (AAM) of marine mammals. The purpose of such monitoring would be to detect marine mammals in those ocean areas where E&P activities are being conducted, in order to allow due diligence in mitigating any potential impact of these E&P operations. The study did not include any direct experimentation.

The AAM study encompassed multiple work components. First, the problem domain was delineated in an overview of offshore E&P activities and of the ocean environments in which they are conducted. To make the analysis more concrete, six specific ocean areas of relevance to E&P were selected and their properties described. Next, the potential performance of AAM was investigated via a parametric study of the sonar equation, incorporating available knowledge of sonar technology and environmental effects (e.g., high-frequency backscattering from the ocean boundaries). This part of the study was intended to identify any fundamental limitations to AAM as imposed by technology or by the basic physics of the problem, and also to pinpoint those sonar features that are of key importance for AAM. Special effort was dedicated to investigating the target strength of marine mammals, as this is an area in which scientific knowledge is sparse at present. The parametric analysis included several generic examples, and was also applied to the six specific ocean areas; however, computer modeling of the six environments was beyond the scope of the study.

This report (Volume V) reviews the factors impacting the performance of an AAM system. The basis of discussion is the sonar equation, with particular attention paid to the scattering properties of marine mammals.

This page intentionally left blank.

Executive summary

Survey of Active Acoustic Monitoring (AAM) Technologies: Volume V: Active Sonar Performance Factors

B. Maranda; L. Gilroy; J. Theriault; E. MacNeil; DRDC Atlantic ECR 2010-044; Defence R&D Canada – Atlantic; March 2010.

Background: Under the Exploration and Production (E&P) Sound and Marine Life Programme, a research study was carried out on the feasibility of the Active Acoustic Monitoring (AAM) of marine mammals. The purpose of such monitoring would be to detect marine mammals in those ocean areas where E&P activities are being conducted, in order to allow due diligence in mitigating any potential impact of these E&P operations. The study did not include any direct experimentation.

Results: The AAM study encompassed multiple work components. First, the problem domain was delineated in an overview of offshore E&P activities and of the ocean environments in which they are conducted. To make the analysis more concrete, six specific ocean areas of relevance to E&P were selected and their properties described. Next, the potential performance of AAM was investigated via a parametric study of the sonar equation, incorporating available knowledge of sonar technology and environmental effects (e.g., high-frequency backscattering from the ocean boundaries). This part of the study was intended to identify any fundamental limitations to AAM as imposed by technology or by the basic physics of the problem, and also to pinpoint those sonar features that are of key importance for AAM. Special effort was dedicated to investigating the target strength of marine mammals, as this is an area in which scientific knowledge is sparse at present. The parametric analysis included several generic examples, and was also applied to the six specific ocean areas; however, computer modeling of the six environments was beyond the scope of the study.

This Volume provides a technical basis for considering the performance of AAM systems. The active sonar equation is presented. The impact of system parameters and the environment are considered through the discussion. Particular attention is paid to the target echo strength. With little known of the acoustic scattering from marine mammals, target strength models are employed to investigate the phenomena.

Significance: The study documents the feasibility of using AAM technologies for mitigating potential impacts of E&P acoustic emissions on marine mammals. There exist technologies that could provide a basis for actively detecting marine mammals between 500 and 1000 m. This Volume presents the analysis which could be used for evaluating specific design features.

This page intentionally left blank.

Table of contents

Abstract …….. i
Executive summary iii
Table of contents v
List of figures vii
List of tables viii
1 Introduction 1
1.1 Background 1
1.2 Document Objective and Structure 1
2 Potential Performance of AAM systems 2
2.1 Introduction 2
2.2 The sonar equation 2
2.2.1 Noise-limited conditions 3
2.2.2 Reverberation-limited conditions 3
2.2.3 Combined equation for signal excess 4
2.3 Source level 5
2.3.1 Definition of directivity 5
2.3.2 Transmit directivity in AAM 5
2.4 Transmission loss 6
2.4.1 Geometrical spreading loss 6
2.4.2 Absorption loss 7
2.5 Target strength 8
2.6 Noise level 8
2.7 Array gain 9
2.7.1 Definition 9
2.7.2 Receiver directivity in AAM 9
2.7.3 Array geometries 9
2.7.3.1 Linear array 9
2.7.3.2 Cylindrical array 10
2.7.4 Numerical values 10
2.8 Detection threshold 11
2.8.1 Noise-limited conditions 11
2.8.2 Reverberation-limited conditions 12
2.9 Scattering strength 12
2.9.1 Theory 12
2.9.2 Empirical data 13
2.10 Factors affecting AAM performance 13
2.10.1 Minimum range capability 14

2.10.2 Waveforms 14
2.10.3 Classification 15
2.10.3.1 Potential methods of classification in AAM 15
2.10.3.2 Rejection of fixed clutter 16
2.10.3.3 Target imaging 17
2.10.3.4 Other considerations 17
2.11 Optimum frequency for AAM sonar 17
2.11.1 Frequency-dependent terms 17
2.11.2 Transducer size 19
2.11.3 Cavitation 19
2.11.4 Target strength of clutter objects 20
2.11.5 Effects on mammals 21
2.11.6 Conclusion on optimum frequency of operation 21
2.12 Worked examples of performance analysis 22
2.12.1 Example 1: Noise-limited conditions 22
2.12.2 Example 2: Surface reverberation 24
2.12.3 Example 3: Bottom reverberation 25
2.12.4 Example 4: Doppler processing 27
2.12.5 Example 5: Shadow zone 29
3 Target Strength 31
3.1 Target Strength 31
3.2 Measured TS 31
3.2.1 Humpback Whale 32
3.2.2 Gray Whale 32
3.2.3 Sperm Whale 32
3.2.4 Dolphin (Atlantic Bottlenose) 33
3.3 Predicting TS 33
3.4 BASIS Models 33
3.4.1 Whale Lung BASIS Model 34
3.5 AVAST 35
3.5.1 AVAST Model 36
3.5.2 Dolphin TS 38
4 Summary 40
References... 43
Distribution list 45

List of figures

Figure 1. The absorption coefficient as computed by the formulas of Thorp and of Mellen et al. For the latter, the parameters are set at d=0.1 km, pH=8.0, t_W=4°C, and S=35 ppt. 8

Figure 2: The frequency-dependent component of the loss (excluding geometrical spreading loss but including two-way absorption loss). Curves are given for different target ranges. 19

Figure 3: The figure of merit for the target strength for a target at 1 km range. If the actual target strength exceeds the figure of merit, the signal excess is positive. Parameters for the three cases appear in Table 3. 23

Figure 4: Maximum depth in the sonar's field of view at a slant range of 1000 m for various beam depression angles and vertical beam widths. The sonar is assumed to be at the surface. 26

Figure 5: Vertical angle subtended at the sonar by a target and the ocean bottom, both at a slant range of 1000 m. The sonar is located at the ocean surface. The curves correspond to three different water depths. 27

Figure 6: Schematic ray diagram of a shadow zone in a downward-refracting ocean. It is assumed that the sound energy is strongly attenuated by the ocean bottom. 30

Figure 7: Boundaries of the shadow zone for a downward-refracting gradient of 0.1 per sec. 30

Figure 8: Humpback Whale 32

Figure 9: Gray Whale 32

Figure 10: Sperm Whale 32

Figure 11: Atlantic Bottlenose Dolphin 33

Figure 12: BASIS Results for Whale Target Strength 34

Figure 13: BASIS Model Based on Lungs 35

Figure 14: AVAST Gray Whale Model 37

Figure 15: AVAST Gray Whale Target Strength Prediction 37

Figure 16: Geometric Gray Whale Model with Lungs 38

Figure 17: AVAST Dolphin TS Estimate 39

List of tables

Table 1: Coefficients in the Mellen-Scheifele-Browning model of sound absorption. 7

Table 2: Array gain, or directivity index, assuming an ideal beam pattern (in dB). 11

Table 3: Parameters used for Example 1. 22

Table 4: Parameters used for reverberation examples. 24

Table 5: Figure of merit for target strength in surface reverberation. 25

Table 6: Figure of merit for target strength in bottom reverberation. Range is 1000 m. 25

Table 7: Figure of merit for target strength in bottom reverberation with Doppler processing of 4-kt target. Range is 1000 m. 29

Table 8: BASIS Parameters for Whales 34

Table 9: Ellipsoid Lung Parameters 35

Table 10: Ellipsoid Lung Parameters 39

1 Introduction

1.1 Background

The International Association of Oil and Gas Producers (OGP) established the Exploration and Production (E&P) Sound and Marine Life Programme as an industry research fund supporting research into sound produced during E&P activities and its effect on marine life.

The JIP (Joint Industry Programme) has funded a proposal by Defence R&D Canada Atlantic, in partnership with Akoostix Inc., to deliver this study which has completed a review and inventory of current active acoustic methods and technologies and has identified potential further development areas for the detection of marine mammals during E&P activities offshore. The study has been approached as a three phase project; during the first phase background information was gathered on E&P activities / environments and a general assessment was done on the performance capabilities of active acoustic technology. In the second phase a survey of manufacturers of active systems was conducted. During the third phase these survey responses were evaluated for suitability of use in monitoring marine mammals at sea during E&P activities and recommendations were made on further development areas.

The study proposal details are contained in response to Request for Proposals JIP08-05.

1.2 Document Objective and Structure

This report is the final report for contract JIP08-05. The report (Volume V) is the last of the series of five volumes.

- Volume I contains an overview and summary of the survey and analysis. Annex B to Volume I includes a Microsoft Excel file, with the detailed responses from each of the system suppliers, along with the evaluation.

- Volume II is the complete contract proposal.

- Volume III is the complete sub-contract report from Canadian Seabed Research on E&P Operations.

- Volume IV is a detailed description of six chosen E&P environments and the marine mammal species expected in those environments.

- Volume V (this document) is a detailed analysis of the factors affecting the performance of an AAM system.

2 Potential Performance of AAM systems

2.1 Introduction

In this volume of the report, a high-level analysis of the potential performance of AAM systems is carried out. The fundamental limits on how well such systems can perform are determined by the laws of physics, but there are also softer constraints imposed by engineering and operating costs, ethical considerations (e.g., allowable active-signal levels to be used against marine mammals in an AAM system), concepts of operation, etc. The following investigation will be guided largely by the physics, taking into account the practical lessons learned at DRDC Atlantic through many years of experience with sonar.

The fundamental purpose of an active sonar is to emit a pulsed signal and detect any return echoes, these echoes being embedded in ambient noise and reverberation. The latter two cases are quite different in nature. On the one hand, when ambient noise is the limiting factor, the performance can be improved by increasing the pulse energy (for example, by increasing the transmitted power, or source level). On the other hand, performance cannot be improved in reverberation-limited environments by raising the source level, because the reverberation level increases proportionately. Instead, improving performance against reverberation may require shaping the transmitter or receiver beam patterns to reduce boundary interaction, employing waveforms with anti-reverberant properties, and exploiting advanced or adaptive signal-processing techniques.

The rest of this Section is organized as follows. First, the sonar equation is given for both noise-limited and reverberation-limited conditions. Then, the various terms that make up the sonar equation are described in more detail, focussing on the operating regime that would be of most interest for an AAM design. It should be noted that only certain terms of the sonar equation are under the direct control of the system designer, although those terms that are determined by the environment may depend on the choice of sonar frequency. Following the basic material on the sonar equation, there is a discussion of higher-level sonar functions such as classification. The issues involved in selecting a frequency for AAM are then examined. Finally, several examples of performance prediction are worked through.

The references [1]-[4] will be drawn upon throughout the discussion, often without specific citation, and references to other material will be made as required. In the following, the terms “long range” and “short range” will be understood in the context of the AAM application, with long range being 1000 m and beyond, and short range being a few hundred meters. Also, for sample calculations it will be assumed that the speed of sound in sea water is $c = 1500$ m/s.

2.2 The sonar equation

A rough prediction of detection performance can be obtained from the sonar equation, which provides an estimate of the signal excess (or echo excess). The signal excess SE is the amount by which the signal-to-noise ratio (or the signal-to-reverberation ratio) at the detector input exceeds the detection threshold, and when SE ≥ 0 the sonar system will meet or exceed the desired level of performance. We now consider separately the form of the equation for noise-limited and for

reverberation-limited conditions, assuming in both cases a monostatic active sonar. As a general notational convention, a term in capital roman letters (e.g., SE, TS) is on a decibel (dB) scale, while a term in math font (e.g., c, T) is in linear MKS units.

2.2.1 Noise-limited conditions

The signal excess SE_N for noise-limited conditions is given by the sonar equation

$$\mathrm{SE}_N = \mathrm{ESL} + \mathrm{TS} - 2\,\mathrm{TL} - \mathrm{NL} + \mathrm{AG} - \mathrm{DT}, \tag{1}$$

where the variables are defined as:

ESL – the *energy source level* of the sonar pulse at a distance 1 m from the acoustic center of the radiating source (an energy level in dB re 1 μPa^2-s at 1 m);
TS – the *target strength* (in dB);
TL – the one-way *transmission loss* between the sonar and the target (in dB);
NL – the *noise spectrum level* at the receiver (in dB re 1 μPa^2/Hz);
AG – the *array gain*, which is the improvement in signal-to-noise ratio provided by the directivity of the sensor system relative to an omni-directional hydrophone (in dB). The array gain is often called the *directivity index* (DI) when the noise is isotropic.
DT – the *detection threshold*, or signal-to-noise ratio required by the detector to achieve a specified level of performance (in dB).

For a flat-topped pulse, the ESL is related to the *source level* SL (having units dB re 1 μPa^2 at 1 m) via the equation

$$\mathrm{ESL} = \mathrm{SL} + 10\log T,$$

where T is the time duration of the pulse (in seconds). Although transducers are usually characterized in terms of SL, it is often convenient to work directly with ESL, because then the effect of pulse shaping, etc, can be handled cleanly.

2.2.2 Reverberation-limited conditions

The form of reverberation that will most likely pose difficulties for the AAM application is reverberation from the ocean boundaries; for example, surface reverberation may be the dominant interference when it is intended that the sonar should detect near-surface marine mammals. This type of reverberation will be assumed in what follows, as the notational changes needed for volume reverberation are minor.

To derive a simplified sonar equation for reverberation-limited conditions, we begin by defining the *echo level* from the target at the sonar receiver,

$$\mathrm{EL} = \mathrm{SL} - 2\,\mathrm{TL} + \mathrm{TS}.$$

The units are those of power, dB re 1 μPa^2. For surface reverberation, the *reverberation level* is given by

$$\mathrm{RL} = \mathrm{SL} - 2\,\mathrm{TL} + \mathrm{S} + 10\log A,$$

where S is the scattering strength, and A is the area of the surface patch that scatters the incident waveform back to the receiver. In writing this equation, the simplifying assumption has been made that the reverberant patch is near the target, so that the two-way transmission loss is the same as for the target echo. The level of the echo above the reverberation is then given by

$$\mathrm{EL} - \mathrm{RL} = \mathrm{TS} - \mathrm{S} - 10\log A,$$

where the transmission loss has cancelled out. The source level has also cancelled out, an indication of the fact that, once the source level has become high enough to cause reverberation to be the limiting factor, increasing it has no effect on the echo-to-reverberation level. The signal excess SE_R for reverberation-limited conditions is now given by

$$\mathrm{SE}_R = \mathrm{TS} - \mathrm{S} - 10\log A - \mathrm{DT}. \tag{2}$$

Details on the computation of the patch size A are provided in a later subsection on the scattering strength S.

2.2.3 Combined equation for signal excess

In the two preceding subsections, separate equations were given for the signal excess in noise- and reverberation-limited conditions. Although it is often useful to analyze the two cases separately in order to identify the dominant effect in a given environment, for carrying out systems analysis it is usually more convenient to have a single equation that combines the effects of both noise and reverberation. Based on the above theory, the following equation can be derived:

$$\mathrm{SE} = \mathrm{ESL} + \mathrm{TS} - 2\,\mathrm{TL} - ((\mathrm{NL} - \mathrm{AG}) \oplus \mathrm{RL}_0) - \mathrm{DT}, \tag{3}$$

where

$$\mathrm{RL}_0 = \mathrm{ESL} - 2\,\mathrm{TL} + \mathrm{S} + 10\log A. \tag{4}$$

In Eq. (3), the symbol $\oplus$ indicates a power summation. That is, given two decibel values $\mathrm{X} = 10\log x$ and $\mathrm{Y} = 10\log y$, their power sum is defined as

$$\mathrm{X} \oplus \mathrm{Y} = 10\log(x + y) = 10\log(10^{\mathrm{X}/10} + 10^{\mathrm{Y}/10}). \tag{5}$$

Similarly, if multiple types of reverberation are present (e.g., surface and bottom reverberation), the separate components should be added in power.

2.3 Source level

2.3.1 Definition of directivity

For an omni-directional acoustic projector, the source level in dB re 1 μPa^2 at 1 m is given by

$$\mathrm{SL}_o = 170.8 + 10\log P,$$

where P is the total radiated power in watts. When the transmitter has directivity index DI_t, the source level on the maximum response axis is

$$\mathrm{SL} = \mathrm{SL}_o + \mathrm{DI}_t = 170.8 + 10\log P + \mathrm{DI}_t .$$

In order to define the directivity more precisely, let a spherical coordinate system be set up with θ being the azimuthal angle (in the horizontal plane) and ϕ the vertical angle measured from the horizontal ($0 \le \theta \le 2\pi$ and $-\frac{1}{2}\pi \le \phi \le \frac{1}{2}\pi$). We denote by $b_t(\theta,\phi)$ the transmit beam power response, normalized such that it has value 1 on the maximum response axis (MRA); then

$$\mathrm{DI}_t = 10\log \frac{4\pi}{\int_0^{2\pi}\int_{-\pi/2}^{\pi/2} b_t(\theta,\phi)\cos\phi \, d\phi \, d\theta}. \tag{6}$$

Here we have used the fact that the element of solid angle is given in the spherical coordinates by $d\Omega = \cos\phi \, d\phi \, d\theta$. The source level quoted for a sonar system usually pertains to that on the MRA.

2.3.2 Transmit directivity in AAM

It may not be feasible to employ any significant azimuthal directivity in AAM on transmit when the goal is to have full azimuthal coverage, since the scan time would be excessive. Note that it is necessary to leave the transmitter off during the time interval that an echo can be received, assuming the usual situation in which the receiver would be overloaded during a transmission from a co-located projector. (Also, in many sonars the same transducer functions as both transmitter and receiver, and is switched between modes.) For a maximum range scale of 1500 m (allowing a 500-m guard band beyond a desired 1000-m detection range), the required observation time on receive would be (2)(1500 m) / (1500 m/s) = 2 s. Then if there are 20 horizontal beams (say), the total scan time would be (20)(2 s) = 40 s. This is probably too long: if the ship were moving at 4 m/s (approx 8 kt), it would advance 160 m during the scan time. If simultaneous operation of the transmit and receive functions could be achieved it would theoretically be possible to step through the scanning pattern more quickly, although frequency diversity or code diversity might be required in order to disambiguate the echoes at the receiver.

Although horizontal directivity on transmit may not be desirable in AAM operations, vertical directivity would be of benefit, because focussing most of the transmitted energy away from the ocean boundaries would reduce the reverberation level. We now outline some of the issues involved. First, if there were no capability for vertical beam steering, the vertical beam pattern would have to be designed to always insonify the sea surface in order to detect near-surface

mammals. In this case, the main benefit provided by vertical directivity would be to reduce or eliminate bottom reverberation in moderately shallow water. If the capability existed for vertical beam steering, additional possibilities would arise; for example, when searching for mammals at depth, it might be possible to steer downward enough to largely avoid insonifying the surface and therefore to eliminate random sea-surface clutter.

2.4 Transmission loss

The transmission loss (TL) is a measure of the sound intensity that is lost by the signal as it propagates through the ocean medium.[=] For the purpose of analysis, it is convenient to break up the transmission loss into two components: that due to geometrical spreading (or focusing) of the sound waves, and that due to absorption. The first component is a propagation effect governed by the acoustic wave equation; the second is a local absorption loss whose functional form has been determined primarily through empirical measurements. A simple model that is often used in practice for short-range transmission loss is given by the formula

$$\mathrm{TL} = 20\log r + \alpha r, \tag{7}$$

where r is the range in meters and α is the absorption coefficient. More specific detail is provided in the following subsections.

2.4.1 Geometrical spreading loss

In a hypothetical ocean in which there were no boundaries, the intensity of the sound issuing from a compact source would decrease according to the inverse square law (or spherical spreading law), as given by the $20\log r$ term in Eq. (7). It is usually accurate to assume spherical spreading at short ranges in the deep ocean, although when the sonar projector is close to the ocean surface — as it would be for many of the sonar systems having potential application to AAM — there are usually surface-related effects. In shallow water, the ocean boundaries can have a profound effect even at short ranges. It is not possible to make a general statement concerning the amount of transmission loss in shallow water, since there are cases where TL will be greater (i.e., worse) than spherical spreading, and other cases where it will be less.

For computing more accurately how sound propagates in a specific ocean environment, one employs propagation models to numerically solve the acoustic wave equation [5]. There are several standard models available to the research community, appropriate for different frequency regimes and providing differing levels of accuracy. At the high frequencies that would be of interest for the AAM application, one would not attempt to predict propagation effects with a range resolution on the order of a wavelength, for it would be impossible to measure the properties of the ocean waveguide itself with such resolution (and many of these properties are time-varying). For performance studies it is generally sufficient to compute range-averaged results on a much coarser distance scale.

[=] The term propagation loss is often used interchangeably with the term transmission loss.

2.4.2 Absorption loss

On a decibel scale the absorption loss is written as αr, where α is the absorption coefficient and r is the range. Many researchers have developed empirical models for the absorption of sound in sea water. The absorption coefficient depends on such environmental parameters as temperature, salinity, etc, but for "back of the envelope" calculations the simplified formula by Thorp (quoted in [1]) is often used:

$$\alpha = \frac{0.1 f^2}{1+f^2} + \frac{40 f^2}{4100+f^2} + (2.75\times 10^{-4}) f^2 + 0.003, \tag{8}$$

where α is in dB/kyd and f is the frequency in kHz. (Dividing this formula by 0.9144 will convert to dB/km.)

A much more complete model can be found in [6]. The formula developed there comprises three terms of the same functional form,

$$\alpha = \frac{S}{35}\sum_{n=1}^{3} \frac{a_n f_n f^2}{f^2 + f_n^2}, \tag{9}$$

with each term accounting for a different physical loss mechanism. The coefficients S, a_n, and f_n are given in the following table:

Table 1: Coefficients in the Mellen-Scheifele-Browning model of sound absorption.

S - water salinity in parts per thousand (ppt)	
$a_1 = 0.5\times 10^{-d/20}$	$f_1 = 50\times 10^{t_W/60}$
$a_2 = 0.1\times 10^{(\mathrm{pH}-8)}$	$f_2 = 0.9\times 10^{t_W/70}$
$a_3 = 0.03\times 10^{(\mathrm{pH}-8)}$	$f_3 = 4.5\times 10^{t_W/30}$
d - water depth in km pH – the chemical pH of the water t_W – water temperature in deg C	

Curves of the absorption coefficient α as given by the Thorp and Mellen formulas (with the former converted to dB/km) are plotted in Figure 1. It is notable that there is a fair amount of difference between the curves, with Thorp's formula yielding an attenuation about 10 dB/km larger at 100 kHz — a difference that is by no means negligible. We shall use the formula of Mellen et al, which should be the more accurate when the parameters properly characterize the water mass of interest.

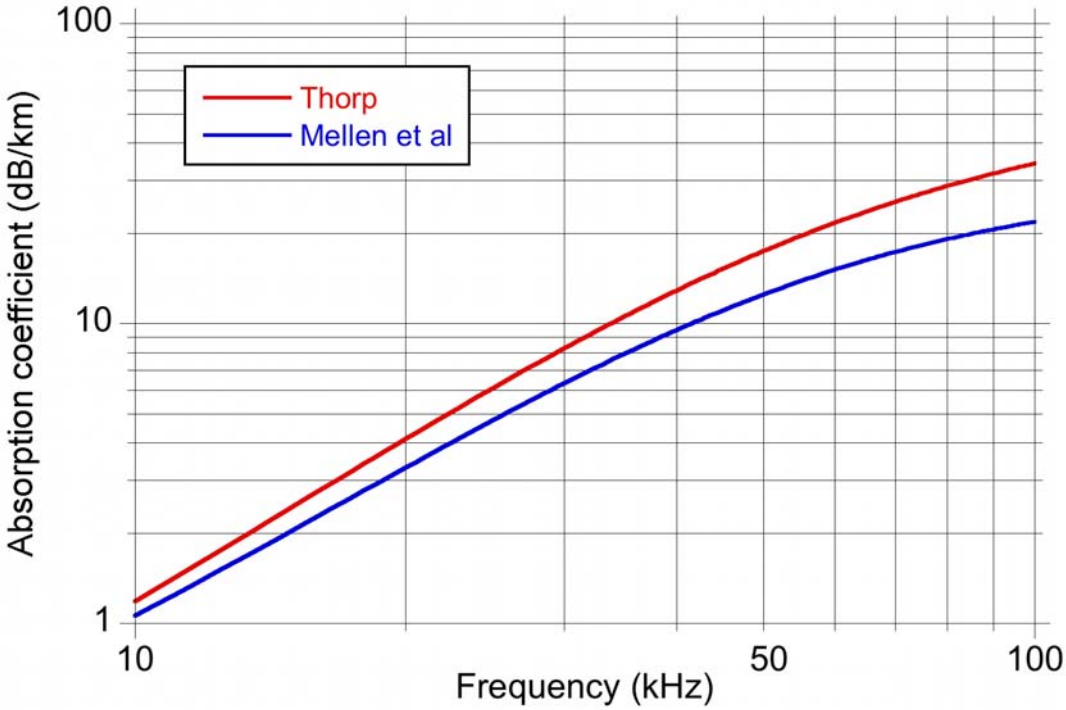

Figure 1. The absorption coefficient as computed by the formulas of Thorp and of Mellen et al. For the latter, the parameters are set at d=0.1 km, pH=8.0, t_W=4°C, and S=35 ppt.

2.5 Target strength

A large uncertainty in evaluating the general performance of an active system in the AAM context is the target strength [Eqs. (1) and (2)]. Under this study, the investigation of the target strength of marine mammals has been afforded extra effort. For this reason, the target strength discussion is included as a self-contained section (Section 3).

2.6 Noise level

Ocean ambient noise is often the limiting factor to sonar detection performance, and as such it has been extensively studied. Although the description of ambient noise is complex at the low frequencies important for military passive sonar, its behavior is much simpler at the frequencies of interest for AAM. In particular, wind is the main causative factor in the generation of ambient noise starting from several kilohertz up to frequencies where thermal noise begins to dominate. The ambient noise in this frequency range typically decreases at a rate of 5 to 6 dB per octave, resulting in lower noise levels at higher frequencies. The frequency at which the thermal-noise component begins to dominate the total ambient noise depends on the sea state. Urick has published an extensive study on ambient noise [7], and he presents a graph (p. 2-29) from which noise levels can be extracted for parametric analysis of sonar performance.

2.7 Array gain

2.7.1 Definition

The array gain, AG, is a measure of how much processing gain is provided by the receiver directivity when in the presence of ambient noise. However, the receiver directivity is also instrumental in reducing the deleterious effects of reverberation, and hence a complete array design should take reverberation into account as well (see Sec. 2.9). For 3D-isotropic noise, the array gain is often called the directivity index; we write DI_r in order to distinguish the directivity index on receive from that on transmit. The formula for DI_r is identical to Eq. (6), except that it is based on the receive beam power response $b_r(\theta,\phi)$:

$$\mathrm{AG} = \mathrm{DI}_t = 10\log\frac{4\pi}{\int_0^{2\pi}\int_{-\pi/2}^{\pi/2} b_r(\theta,\phi)\cos\phi\, d\phi\, d\theta}. \tag{10}$$

Like the transmit response, the receive response $b_r(\theta,\phi)$ is normalized so that it has unity value on its maximum response axis.

2.7.2 Receiver directivity in AAM

In what follows, it is assumed that the receiver directivity is realized by the formation of steered beams. In order to provide adequate processing gain, and also to provide the capability of mapping target detections in the horizontal plane, an AAM sonar will require substantial horizontal directivity on receive; that is, the beamwidth must be narrow in azimuth. A narrow azimuthal beamwidth would also be advantageous in combating reverberation. For this scheme to work, however, all receive beams must be processed in parallel; the alternative, to scan through the beams individually, was ruled out for transmission (see Sec. 2.3.2), and the same reasoning applies to reception. Moreover, real-time beam stabilization would be required in order to exploit narrow beamwidths when the sonar is mounted on a moving platform; those commercial sonars intended for fixed installation would generally not implement beam stabilization owing to its complexity.

As on transmit, vertical directionality on receive would help to reduce surface reverberation if it were possible to steer the vertically away from the surface; however, operating in this manner would no doubt preclude the detection of near-surface targets. Vertical directionality would also make it possible to reduce or avoid bottom reverberation for targets well separated from the ocean bottom, although if detection coverage is required throughout the entire water column there will be no way to entirely avoid seabed reverberation.

2.7.3 Array geometries

2.7.3.1 Linear array

It is assumed that, for a moving platform, a linear receive array would be oriented with its axis in the direction of motion (along track). The linear array has several disadvantages for the AAM application, as will now be discussed. First, a linear array constructed with omni-directional sensors has an axially-symmetric beam pattern that causes a left / right ambiguity; since this ambiguity would be unacceptable in the AAM application, the use of a linear geometry would

require the exploitation of directional sensors, or the separation of the array into two isolated halves (as can be found in sidescan sonars). Another problem with the linear geometry is that it provides narrow beams near broadside, but considerably wider beams near endfire. Sidescan sonars limit their field of view to angles very close to broadside in order to obtain the desired angular resolution, but for the AAM application a wider field of view would be imperative. In summary, a linear receive array is not well suited for the AAM application.

2.7.3.2 Cylindrical array

The standard array configuration for a hull-mounted sonar is a cylindrical array with its axis oriented vertically. The advantage of the cylindrical geometry is that it can provide the same horizontal beamwidth at all azimuthal steering angles, a property that is desirable for the plan-position indicator (PPI) display used in many sonars. Furthermore, if the same transducer set is used for both transmit and receiver, the cylindrical array will provide a suitable transmit beam pattern. (If the linear array were used as a receiver array, it would likely be necessary to have a separate transducer for transmit.) In summary, the cylindrical geometry provides a compact transducer geometry with desirable features, as evidenced by the prevalence of this geometry in many fish-finding and swimmer-detection sonars.

2.7.4 Numerical values

To get precise values of DI_r, it would necessary to have an analytical formula for the beam power response of the receiver, and this can be obtained only if an array configuration has been specified. The approach taken here will be approximate: the actual beam response will be replaced by an ideal response that assumes a value of 1 in the mainlobe region, and a value of 0 everywhere else (the sidelobe region). Letting θ' and ϕ' denote the respective horizontal and vertical beamwidths of the mainlobe, the beam response is equal to 1 in the angular region defined by $\theta_0 - \frac{1}{2}\theta' \le \theta \le \theta_0 + \frac{1}{2}\theta'$ and $-\frac{1}{2}\phi' \le \phi \le \frac{1}{2}\phi'$, where the azimuthal steering angle is θ_0 and the vertical steering angle is taken to be zero. The angles θ' and ϕ' are the *noise-equivalent beamwidths* when they yield a directivity index for the ideal response that is equivalent to that of the actual response. The noise-equivalent beamwidths are wider than the –3 dB beamwidths, which are the figures usually quoted. Analytically, we obtain

$$\mathrm{DI}_r = 10\log\frac{4\pi}{\int_{\theta_0-\theta'/2}^{\theta_0+\theta'/2}\int_{-\phi'/2}^{\phi'/2}\cos\phi\, d\phi\, d\theta} = 10\log\frac{2\pi}{\theta'\sin(\phi'/2)}. \tag{11}$$

When ϕ' is small, the argument of the logarithm is approximately $4\pi/\theta'\phi'$; that is, the solid angle of the beam is approximated by a rectangle of sides θ' and ϕ'. Equation (11) was used to compute the directivity index for a set of horizontal and vertical beamwidths that is believed to be representative of the parameters possible for AAM sonars (refer to Table 2). It can be seen from the table that a considerable processing gain in 3D ambient noise would be available for the AAM application.

Table 2: Array gain, or directivity index, assuming an ideal beam pattern (in dB).

		Equivalent azimuthal beamwidth				
		2°	4°	6°	10°	15°
Equivalent vertical beamwidth	10°	33.1	30.1	28.4	26.2	24.4
	20°	30.2	27.1	25.4	23.2	21.4
	30°	28.4	25.4	23.7	21.4	19.7
	40°	27.2	24.2	22.4	20.2	18.5
	50°	26.3	23.3	21.5	19.3	17.5

2.8 Detection threshold

The detection threshold is a measure of the signal-to-noise ratio or of the signal-to-reverberation ratio that is required by the sonar processor to achieve a specified detection performance. As outlined in texts on detection theory [8],[9], it is necessary to specify the performance in terms of both the probability of detection, P_d, and the probability of false alarm, P_{fa}. One approach to adjusting the sonar system during operation is to set P_{fa} such that the operator can cope reasonably well with the resulting number of false alarms.

2.8.1 Noise-limited conditions

The optimum processor for detecting a signal against a background of additive white Gaussian noise is the matched filter. In an AAM sonar the signal will be a bandpass signal of unknown phase, and the filter should be followed by an envelope detector. For a CW signal, the matched-filter detector is approximated very well by the traditional detector consisting of a rectangular bandpass filter followed by an envelope detector. For FM signals, implementing the matched filter requires significantly more computational resources. The properties of different waveforms are discussed in Sec. 2.10.2.

The detection threshold is given by $\mathrm{DT} = 10\log\gamma$, where γ is the signal-to-noise ratio (SNR). Here $\gamma = E/N_0$, where E is the pulse energy (in μPa^2-s) and N_0 the power spectral density of the ambient noise (in μPa^2/Hz), both being measured at the detector input. The detector output in this case has a chi-square distribution with two degrees of freedom, and the detector performance is given by the equation (p. 345 of [8])

$$P_d = Q\left(\sqrt{2\gamma}, \sqrt{-2\ln P_{fa}}\right) \tag{12}$$

where Q denotes the Marcum Q-function. A graph of P_d as a function of SNR for various values of P_{fa} can be found on p. 205 of [9].

It should be noted that, on the one hand, the detection theory presented here assumes white noise (i.e., a flat noise spectrum), but, on the other hand, the actual noise spectrum is expected to roll off at a rate of 5 to 6 dB per octave. The technical solution would be to pre-whiten the sloped noise by placing an appropriate filter before the matched filter; however, the fractional

bandwidths of sonar signals used above 10 kHz are generally so small that the noise spectrum level over the matched-filter bandwidth is adequately represented by a single number.

2.8.2 Reverberation-limited conditions

The theory of detection in reverberation is not as well worked out as it is for Gaussian noise, but it will still be assumed that the matched-filter envelope detector is used. A common physical model is that the reverberation arises from a large number of scatterers distributed randomly throughout the scattering region. Mathematically, this model leads to Rayleigh-distributed reverberation; that is, the detection statistics are chi-square with two degrees of freedom. Therefore Eq. (12) still holds, but now γ is to be interpreted as the echo-to-reverberation ratio at the output of the matched filter.

2.9 Scattering strength

2.9.1 Theory

The scattering strength S is a quantitative measure of the amount of acoustic power scattered from an insonified area or volume. Clearly it is similar in definition to target strength, except that we are now dealing with a distributed surface or volume that is scattering unwanted (interfering) power. In what follows, surface scattering is considered. For analytical convenience the scattering parameter S pertains to a unit area (m^2), the total scattering power then being derived from the scattering area A actually insonified by the sonar pulse. The formula for A is

$$A = \frac{cT}{2}\Theta r,$$

where c is the speed of sound, Θ is the effective azimuthal beamwidth, and r is the range. Note that the pulse duration T is used when the pulse is a gated CW signal; for a swept FM signal processed with a matched filter, the pulse duration should be replaced by the compressed duration of the pulse. Since the compressed duration is approximately given by the inverse of the swept bandwidth W, the previous equation is often written in the form

$$A = \frac{c}{2W}\Theta r, \tag{13}$$

applicable for both CW and FM signals. According to this equation, a doubling of the waveform bandwidth will improve detection performance in reverberation-limited conditions by 3 dB. In practice, one cannot reap continual improvement by expanding the bandwidth because (1) the target becomes over-resolved, and (2) the coherence of the signal is degraded as it propagates through the ocean medium. Further discussion of waveform design is presented later.

The effective beamwidth Θ for reverberation calculations depends on both the transmit and receive beam responses:

$$\Theta = \int_0^{2\pi} b_t(\theta,\phi_0)\, b_r(\theta,\phi_0)\, d\theta, \tag{14}$$

where ϕ_0 is the vertical angle between the projector and the insonified patch on the ocean boundary (equal to the grazing angle). When the sonar system is located near the surface, we have $\phi_0 \approx 0$ for sea-surface reverberation; that is, the reverberation performance is determined by the beam responses close to the horizontal plane. For bottom reverberation, the value of ϕ_0 would be derived from the geometry of the problem. Note that the value of ϕ_0 changes as a function of time after the transmission of a ping.

2.9.2 Empirical data

Field measurements have been made for many years in order to determine numerical values for the scattering strength S. For scattering from the ocean surface, the main parameters on which S depends are the grazing angle, the wind speed (which determines the surface roughness), and the frequency. For frequencies below 10 kHz, an empirical formula derived by Chapman and Harris is commonly used to predict the scattering strength [1]. At the higher frequencies of interest for AAM, semi-empirical models for the scattering strength can be found in [10]. Unfortunately, there is uncertainty in the value of S at the low grazing angles that would occur in a typical AAM sonar geometry: measured curves generally do not fall off as rapidly as theory predicts when the grazing angle approaches 0°. McDaniel [11] refers to this behavior as anomalous scatter and attributes it to the presence of microbubbles near the ocean surface. The dependence of the scattering strength on the wind speed is very marked, with S increasing by 30 dB as the wind speed increases from 0 to 10 m/s.

The scattering strength of the ocean bottom depends on the local composition and roughness of the seabed, and hence shows a wide variability from area to area. One difference from sea-surface reverberation is that the anomalous scattering at low grazing angles mentioned above is not seen, as there is no bubble layer. In fact, the authors of a recent book on seafloor acoustics [12] claim that measurements of the scattering strength of the ocean bottom should be viewed with suspicion if they do not fall off rapidly as the grazing angle becomes small. However, for a sonar system located near the ocean surface, as would be likely in the AAM application, the grazing angles at the ocean bottom would usually be much greater than at the surface, implying a large backscattering strength. For long-range detection in shallow or moderately shallow water, it may be difficult to attain enough vertical directivity in the beam pattern to avoid interaction with the ocean floor.

In summary, the scattering strength term of the sonar equation depends strongly on the local environmental conditions, and there is uncertainty in what value to use in performance assessments. This uncertainty will reduce the reliability of predicted signal excess, SE_R.

2.10 Factors affecting AAM performance

The sonar equation is essentially a bookkeeping method for tracking the level of acoustic power throughout the detection scenario, and is only a rough gauge of potential performance. A more careful analysis must account for numerous factors that will ultimately decide the overall utility of the sonar, not merely as means for detection but as a *system* capable of achieving the desired objective. For example, the detections themselves may be of little utility if a method of classification is not available. The following subsections provide some discussion on issues affecting the performance of AAM systems.

2.10.1 Minimum range capability

In monostatic sonars the transmitter and receiver are co-located, and it is generally impossible to provide enough acoustic isolation between them to allow simultaneous transmission and reception. The receiver will be allowed to saturate during transmission, or a gain control will shut the receiver off. In some sonar systems, the transmitter and receiver share the same physical transducer through a transmit/receive (T/R) switch. Regardless of the instrumentation, the effect is to create a blind area (or "dead zone") around the sonar, the minimum range capability being determined by the length of the sonar pulse. For example, if the pulse duration is 100 ms, then the minimum range is (0.1 s)(1500 m/s) / 2 = 75 m.

In practice, the pulse duration can be chosen automatically as the sonar operator changes the range scale on the sonar set. On a short-range setting, a short pulse length would be used in order to minimize the dead zone; on a long-range setting, where it is allowable to expand the dead zone around the sonar, a longer pulse length could be used. This method is well suited for noise-limited conditions, since each doubling of the pulse length adds another 3 dB of energy for longer-range detections. In the AAM application, the concept of operations would have to ensure that a marine mammal couldn't penetrate into the blind area without first being detected in an outer ring; a sector-scanning concept would be vulnerable to this type of problem.

2.10.2 Waveforms

In early sonars, the only type of pulse was a gated sinusoid (also called a continuous-wave, or CW, pulse). The range resolution of such pulses is determined by their duration: short-duration CW pulses provide better range resolution than long-duration pulses simply because the echoes can be closer together in time without overlapping. The problem is that by reducing the pulse duration in order to improve resolution, one also reduces the pulse energy and hence the detection performance in ambient noise. A big step forward was made in signal-processing theory when it was realized that pulse compression via matched filtering can decouple the achievable range resolution from the choice of pulse length. In particular, the amount of compression depends on the signal bandwidth, and hence a long-duration pulse with sufficient swept bandwidth can be compressed to a short time span at the filter output. It is this effect that also makes FM pulses effective in combating reverberation, as described in Sec. 2.9.

For example, suppose the pulse bandwidth is chosen to be 1 kHz. A CW pulse of this bandwidth has a duration of ~1 ms. In contrast, a frequency-modulated (FM) pulse with a 1-kHz bandwidth may have a much longer duration (say 100 ms), but will nevertheless compress to ~1 ms at the output of a matched filter. In this example, two FM echoes arriving 10 ms apart in time (for point targets separated by 7.5 m in range) would be 90% overlapped at the matched filter input, but would still be easily resolved at the filter output. Extension of this reasoning leads to the conclusion that the long FM pulse would provide performance against reverberation similar to that of the short CW pulse. Note, however, that a 100-ms FM pulse would have 20 dB more energy than a 1-ms CW pulse and hence yield much better detection performance in ambient-noise-limited conditions.

More generally, the concept of a pulse's ambiguity function clarifies how both range and frequency (Doppler) resolution are affected by changes in the pulse shape when matched filtering is used. It is with this greater insight that different pulses can be designed to attain different goals; a general rule of thumb is that wideband signals are used for better range resolution and

narrowband signals for better Doppler resolution. The ideal pulse would of course provide high resolution in both dimensions simultaneously, but ambiguity-function theory tells us that there is an unavoidable trade-off between them. In practice the sonar may implement a suite of pulses that have been tailored for various tasks. In order to exploit Doppler-sensitive waveforms (to separate moving contacts from stationary contacts, for example) when the sonar is mounted on a moving platform, the implementation of own-Doppler nullification would be highly desirable.

The use of FM waveforms and matched-filter processing is commonplace in military sonars. However, there remain areas of commercial application where matched filtering has not penetrated the sonar technology to any great extent, and where the term "pulse" almost invariably means a CW pulse. For example, two relatively modern books on fisheries acoustics [13],[14] mention non-CW signals only briefly, and, no doubt reflecting the actual design of fisheries sonars, take it for granted that the pulse duration must be decreased in order to improve the range resolution. This lag in technological development perhaps stems from the difference between the commercial and military worlds, the former being content with a capability adequate for a given task (with one eye firmly on system cost) and the latter striving to field the best capability achievable.

2.10.3 Classification

The basic function of a sonar system is detection. From the standpoint of performing a specific task, such as AAM, the fact that the sonar will indiscriminately detect all objects in its field of view is a complicating factor, which in some conditions can make it impossible to carry out the assigned task. The desired contacts are usually called *targets* and the undesired ones *clutter* or *false alarms*. An important post-detection function is then to distinguish between targets and clutter; i.e., to classify the contacts.

2.10.3.1 Potential methods of classification in AAM

The methods of classification that can be implemented depend on the information being obtained through the sonar sensor; the type and amount of this information will depend not only on the sonar equipment itself, but also on scenario-dependent factors such as target range. If it is desired to classify contacts at long ranges, the majority of marine mammals will effectively appear as a point targets in a beam; that is, the angle subtended by the target (as seen from the receiver) will be smaller than the beamwidth. For example, a narrow beamwidth of only 2° translates into a cross-range distance of 35 m at a range of 1000 m. Clearly the majority of sea animals will appear as point targets (in azimuth) at such ranges.

Although the range resolution would remain good with the appropriate waveforms (1 m or better, say), the range structure of the sonar return would generally not provide reliable classification clues. Some considerations are: (1) There may be multiple, closely spaced mammals within a single beam, and these would all contribute to the range structure in that beam. (2) The aspect angle of each mammal relative to the sonar would usually be random, giving different range structures. (3) Often there are multiple transmission paths in the acoustic channel, giving rise to a channel impulse response that exhibits time spreading; for example, multiple distinct arrivals may show up over a time spread of a few tens of milliseconds. Even if the pulse type allowed fine range resolution, the time spread in the channel impulse response would confuse the picture. This

last comment is most relevant to long-range detection, where the channel impulse response would be more complex; at short ranges, the channel response may be quite simple.

In summary, for initial detection at long range, it cannot be expected that the sonar will provide enough information to permit the classification of a target as a marine mammal on the basis of shape or structure, although this may happen when circumstances are favourable. Naïve concepts of target strength (e.g., bigger targets will have larger target strengths) are also unlikely to lead to reliable methods of classification. A process of elimination leaves target motion as the best source of classification information for long-range detections. The methods that can be used to show the presence of target motion depend on the time-frame allotted for a decision to be made: if only a few pings are allowed, then Doppler-sensitive waveforms are necessary, although these will fail to detect motion for targets moving in the cross-range direction. If one can allot more time to decision-making, then it is sufficient to monitor the time evolution of the target bearing and range, and a waveform that provides an accurate range is more desirable. In this mode of operation, the performance of target trackers becomes important, particularly if the automatic initiation of tracking can help to reduce the operator workload. Another motion-related criterion is the time evolution of a target's extent; for example, a school of fish may appear to change in size in a way that is not consistent with a single marine mammal.

2.10.3.2 Rejection of fixed clutter

During a stationary, long-term deployment of the sonar, it would be possible to learn fixed clutter features (such as those located on the ocean bottom). For a simple sonar system with no adaptive processing, the learning would be done by the sonar operator, who would quickly begin to recognize permanent clutter features and eliminate them from consideration as potential contacts. The feasibility of this approach would depend on the clutter density, as a highly cluttered environment would perhaps place too great a burden on the operator; however, environments in which there are only a few discrete clutter returns should not present any impediment to successful operation, even when the sonar operator is inexperienced. A more complicated sonar system could implement adaptive clutter-reduction algorithms based on the construction of a clutter map, which could be built up over a long period of time and used to normalize the sonar returns. It would be much more complicated to remove fixed clutter when the sonar is moving, since the changing aspect of bottom features would result in large ping-to-ping variability; at high frequencies, even small changes in geometry become significant in this regard.

As another approach, the use of Doppler-sensitive waveforms would allow the use of moving-target processing to remove fixed clutter features. However, such waveforms would not typically be the primary waveform type, for they generally offer lower range resolution than Doppler-insensitive waveforms designed for detection. Hence the Doppler-sensitive waveforms would be used in conjunction with other waveform types, either being sent in tandem with Doppler-insensitive waveforms or being transmitted after a potential detection has been made, when the sonar operator would invoke a moving-target sonar mode. As noted above, for a sonar mounted on a moving platform, some form of own-Doppler nullification would be desirable; otherwise, interpretation by the sonar operator becomes unnecessarily complicated.

2.10.3.3 Target imaging

As a target moves closer to the sonar, eventually a point is reached when the target no longer appears as a point target in a single beam, but instead is extended across multiple, adjacent beams. In such circumstances the sonar provides enough information to "paint" a structured image of the target on the sonar screen. The detection and classification problem then takes on a new flavor, since with a large number of independent beams a recognizable image of the target can be built up even with fairly poor results in each range-and-beam cell. It is the classification using many search cells that makes it possible to declare a detection even when the result from each cell in isolation would be too inconclusive to allow a detection to be called. (An analogy is the use of side-scan sonar for mine detection: one does not call a detection based on a strong return in a single search cell; instead, it is the formation of a recognizable mine-like image that leads to a classification and hence to a called detection.)

Practically speaking, the ability to image a marine mammal with sufficient fidelity to make a classification would be possible only at very short ranges. Though likely to be impractical for E&P applications, an imaging sonar would have to be mounted on an auxiliary watercraft (e.g., a RHIB) that is vectored to a location based on an initial detection from a main sonar. Whether such a concept of operations is possible depends on factors beyond the scope of this study.

2.10.3.4 Other considerations

In some areas of the world, schools of fish could lead to difficulties. If there were many small, detached schools, each one of which looked acoustically like a marine mammal at long range, the false alarm rate could overwhelm the sonar operator. That is, so many potentially valid contacts would continually enter into the sonar's field of view that it would impossible to attempt to classify them all, and it would be necessary either to resolve the problem through other detection modalities (passive, visual) or else to accept the uncertainty. However, it may be considered justifiable in such a scenario to examine a subset of the contacts, and work under the assumption that if those contacts actually classified turn out to be false alarms (fish or other), then it may reasonably be deduced that the unexamined contacts are also of no interest. Whether this latter approach can be deemed reasonable depends on non-scientific factors that lie outside the scope of this discussion. Further discussion on fish as potential contacts can be found in Sec. 2.11.4.

2.11 Optimum frequency for AAM sonar

There are multiple considerations that must be taken into account when assessing the question of what operating frequency (or frequencies) is most suitable for AAM. As is usual in most engineering design tasks, it is necessary to perform a trade-off analysis between a number of competing factors. Since the goal here is not to present a detailed design, we shall restrict ourselves to a general examination of the main factors that enter into the analysis.

2.11.1 Frequency-dependent terms

Sound absorption in sea water increases dramatically as the frequency rises, and will be an important factor in determining the range capability of a sonar at the frequencies of interest for AAM. A counter-balancing effect for noise-limited conditions is that, in the frequency band of interest, the ambient noise will decrease as the frequency rises (until the thermal noise is reached, at which point the trend reverses). In what follows, we shall consider how these two terms trade

off against one another. In a more comprehensive investigation, the frequency dependence of other terms, such as the target strength, would also enter into the analysis; however, at present there does not appear to exist a validated model describing how the target strength of marine mammals varies as a function of frequency.

Note also that we are considering only those terms of the sonar equation that are determined by the ocean environment and which therefore lie outside the control of the sonar designer. At the design stage, one can, within certain physical constraints, ignore the frequency dependence of equipment parameters. For example, the array gain would vary with frequency for a fixed transducer size; however, it can be assumed that AG is fixed while optimizing the frequency of a new design because the size of the transducer would be scaled to yield the desired AG at the frequency selected (see Sec. 2.11.2).

It is seen from Eq. (1) that the signal excess of a received echo will be maximized when the sum $2\,\mathrm{TL}+\mathrm{NL}$ is at its minimum. We shall assume that the transmission loss is of the form in Eq. (7), which is re-written here to indicate its frequency dependence:

$$\mathrm{TL}(f) = 20\log r + \alpha(f)r. \tag{15}$$

The absorption coefficient will be computed using Eq. (9). The noise spectrum will be assumed to roll-off at 5 dB per octave over the frequency band of interest, leading to the formula

$$\mathrm{NL}(f) = \mathrm{NL}_{1\ \mathrm{kHz}} - 16.6\log(f), \tag{16}$$

where f is in kHz and $\mathrm{NL}_{1\ \mathrm{kHz}}$ is the noise spectrum level at 1 kHz. We may now write

$$2\,\mathrm{TL}(f) + \mathrm{NL}(f) = 40\log r + \mathrm{NL}_{1\ \mathrm{kHz}} + J(f), \tag{17}$$

where the frequency-dependent terms have been collected into the function

$$J(f) = 2\alpha(f)r - 16.6\log f. \tag{18}$$

Figure 2 shows curves of this objective function for four different ranges. It is seen from the figure that the curves are at their minimum (i.e., most advantageous for range performance) for the low frequencies, and that they rise significantly as the higher frequencies are reached. At 100 kHz, each range increase of 500 m costs another 20 dB in two-way absorption loss. (Note that the frequency-independent geometric spreading loss is not included in these curves. If it were, the curve for 2.0 km would show an additional 24 dB of two-way loss relative to the curve for 0.5 km.)

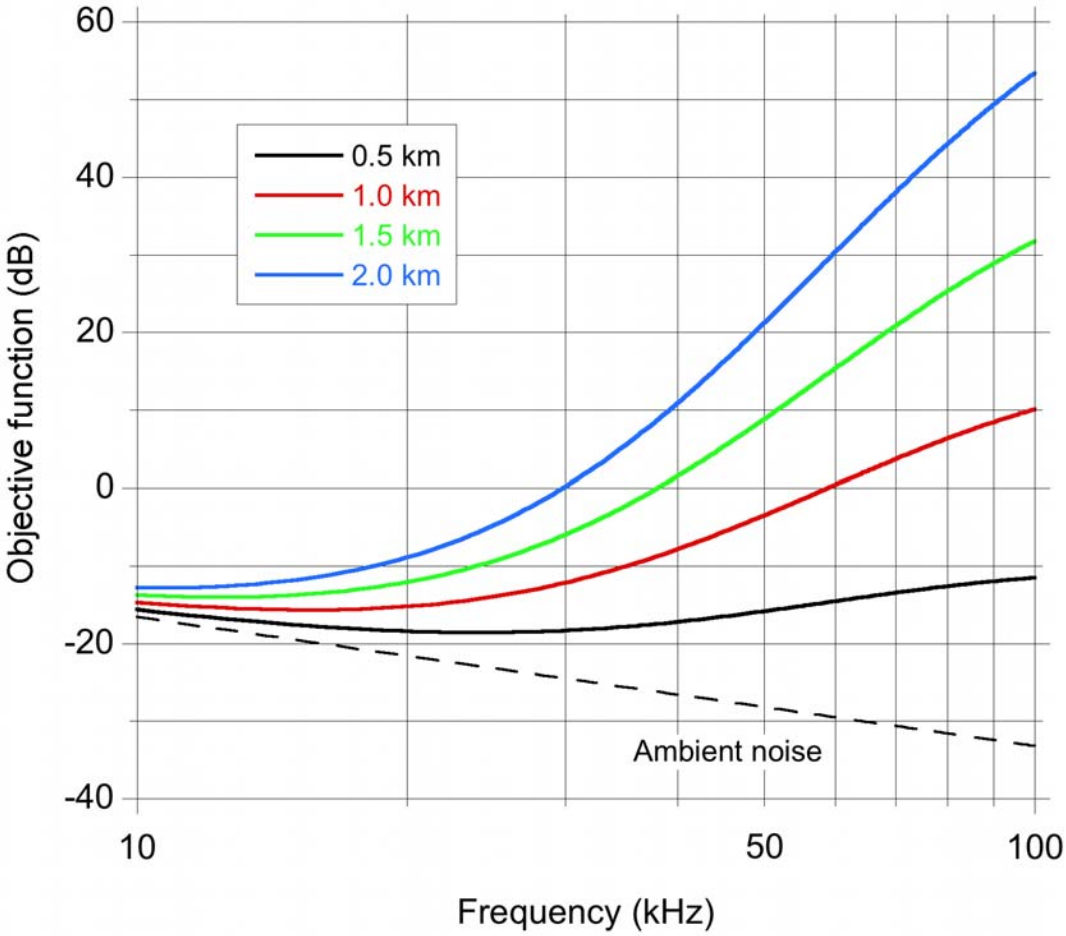

Figure 2: The frequency-dependent component of the loss (excluding geometrical spreading loss but including two-way absorption loss). Curves are given for different target ranges.

2.11.2 Transducer size

The size of the transducer that is required to achieve a given beamwidth depends on the frequency at which the transducer is to operate. If the goal is to achieve a specified beamwidth, a doubling of the wavelength (i.e., halving the frequency) will require a concomitant doubling of the physical dimensions of the transducer. Since increased transducer size and weight translate directly into increased cost – for the transducer itself, for the ship mount or gear required for its installation or deployment, etc – there is an obvious financial inducement to reduce size and therefore work at higher frequencies.

2.11.3 Cavitation

Cavitation at the transducer face is a limitation on the source level that can be achieved by an acoustic projector. The physics is such that the onset of cavitation will occur at higher source

levels with an increase in either the depth or the transmit frequency of the projector. Since it would not be possible to put a hull-mounted AAM sonar very deep (5 to 10 m, say), there will be little depth effect. It is not obvious what effect an increase in frequency would have on the cavitation threshold if the transducer size were scaled with frequency as suggested in the previous subsection. On the one hand, at a higher frequency the transducer face would be able to handle more power per area (W/m^2) before cavitation set in; on the other hand, if the transducer were scaled down in size, its power-handling requirement in W/m^2 would increase if the total radiated power were held constant. Perhaps the best indication of what would be possible for AAM can be obtained through analogy with existing technology. On this basis, cavitation is not expected to impose a limitation on source level for AAM, considering that hull-mounted military sonars are capable of transmitting at very high source levels even at frequencies below 10 kHz.

2.11.4 Target strength of clutter objects

The goal of AAM is to detect marine mammals, which are fairly substantial in size compared to most other scatterers in the water column. It would be beneficial if it could be arranged that the small scatterers that constitute clutter for AAM should have weak or negligible sonar returns. Now, in many cases if a scatterer is small compared to the wavelength of an incident acoustic wave, its backscattered acoustic energy will also be small; that is, its target strength will be low. We state a classic result from the physics of scattering [4]. Let σ_{bs} denote the backscattering cross-section of an object (so that $\mathrm{TS} = 10\log\sigma_{\mathrm{bs}}$ is the target strength), let λ denote the wavelength of the incident acoustic wave, and let $k = 2\pi/\lambda$ be the wavenumber. Lord Rayleigh first proved the following result: for a rigid, fixed sphere of radius a, the ratio of the sphere's backscattering cross-section to its geometric cross-section has the dependence

$$\frac{\sigma_{\mathrm{bs}}}{\pi a^2} \propto (ka)^4$$

when $ka << 1$. This equation shows that when the sphere's radius is small compared to the wavelength of the incident sound, its backscattering cross-section (and hence target strength) falls off very quickly as ka decreases. This exact result holds only for a rigid sphere, but it is generally true that the target strength will be low for a hard object that is small compared to the wavelength (a "Rayleigh scatterer").

An important exception to the above theory is the air bubble, which owing to its compliance may have a scattering cross-section that is orders of magnitude greater than its geometric cross-section even when the bubble radius is much smaller than the wavelength. Thus, although lowering the frequency may help to eliminate returns from certain types of clutter objects in the water column, it would not do much to mitigate strong scattering from bubbles. Although under usual circumstances the highest concentration of bubbles will be in a zone extending a few meters downward from the surface, some species of marine mammals spend most of their time in that zone and hence must be detected there. The bubble wake from other watercraft would also cause sonar returns, and owing to the extinction of sound passing through the wake, in some geometries the wake could act as an acoustic barrier behind which nothing would be seen. This last point may have a bearing upon the concept of AAM operations, for it suggests (1) that detection performance of a hull-mounted sonar will be poor when pointing aft, owing to the ownship wake (setting aside the matter of equipment that is being towed), and (2) any auxiliary watercraft near

the sonar-equipped ship(s) will have to be positioned correctly if adverse wake effects are to be minimized.

The high target strength of air bubbles also implies the strong detectability of those fish that possess swim bladders. Even individual fish with swim bladders may show up on a sonar display, leading to a large amount of clutter; from the point of view of detecting marine mammals, these detections would represent unwanted or false alarms.

In summary, decreasing the sonar frequency would aid in reducing clutter from Rayleigh scatterers, but would not have much effect in combating unwanted returns from air bubbles or from fish with swim bladders.

2.11.5 Effects on mammals

Another consideration when choosing the frequency of operation is whether or not the sonar transmissions could be harmful to marine mammals. One idea would be to choose a frequency that lies outside the hearing response of most marine mammals. (For example, the hearing range of mysticetes may not extend above 20 – 30 kHz, where as some odontocetes are well above that). The question to be answered is this: can an animal be harmed by acoustic energy that lies outside its hearing response? If we exclude from consideration extremely high energy levels (well above the levels produced by standard sonar technology) the answer is likely negative. However, a definitive answer to this question is beyond the scope of this report.

2.11.6 Conclusion on optimum frequency of operation

There are numerous competing factors that arise when attempting to determine the "optimum" sonar frequency for AAM operations. Most of the factors considered above tend to suggest the use of a lower, rather than a higher, frequency; a significant exception is transducer size, which is most favourable for realization at higher frequencies. A reasonable conclusion is that frequencies below about 50 kHz are required for the long-range search phase, although higher frequencies may be of use for short-range classification.

2.12 Worked examples of performance analysis

2.12.1 Example 1: Noise-limited conditions

In the first example, detection performance in ambient noise is evaluated. The starting point for the analysis is Eq. (1) for the signal excess SE_N. If we require that $\mathrm{SE}_N \geq 0$, this equation can be written as a condition on the target strength, namely

$$\mathrm{TS} \geq \mathrm{TS}_{\mathrm{FOM}} \equiv 2\,\mathrm{TL} + \mathrm{NL} - \mathrm{SL} - 10\log T - \mathrm{AG} + \mathrm{DT}. \tag{19}$$

The right-hand side of the inequality defines a figure of merit (FOM) for the target strength; when $\mathrm{TS} \geq \mathrm{TS}_{\mathrm{FOM}}$ the signal excess will be positive. For the calculations that follow, we shall use the simple model for $2\,\mathrm{TL} + \mathrm{NL}$ given in Eq. (17); then

$$\mathrm{TS}_{\mathrm{FOM}} = 40\log r + \mathrm{NL}_{1\,\mathrm{kHz}} + J(f) - \mathrm{SL} - 10\log T - \mathrm{AG} + \mathrm{DT}, \tag{20}$$

where $J(f)$ is the function defined in Eq. (18) and plotted in Figure 2. Three cases will be examined, the parameters for which are given in Table 3. The values of r and $J(f)$ remain unspecified at this point. Case 1 is meant to represent a set of parameters favourable for detection, while Case 2 represents moderate parameters. Case 3 assumes a high noise level corresponding to sea state 6.

Table 3: Parameters used for Example 1.

		Parameter values		
Parameter name	Units	Case 1	Case 2	Case 3
SL	dB re μPa^2 at 1 m	220	215	215
T (pulse length)	s	0.025	0.0025	0.0025
NL at 1 kHz	dB re μPa^2/Hz	60 (sea state 2)	60 (sea state 2)	70 (sea state 6)
AG	dB	24	24	24
DT	dB	12	12	12

Comments are now made on several entries in the Table. First, the pulse length of 25 ms chosen for Case 1 has 10 dB more energy than the short 2.5-ms pulse in Case 2. One would use the shorter pulse length as a means to obtain bandwidth (and range resolution) if the sonar system only had CW capability; otherwise, if FM pulses were available, the desired bandwidth could be obtained with the longer 25-ms length. The array gain of 24 dB was chosen from Table 2 as a figure that should be realizable in practice without much difficulty.

The choice of DT = 12 dB requires a more detailed explanation. We first must specify values for the probabilities of detection and false alarm. Now, if we assume the sonar has 120 beams in azimuth and 1500 range cells per beam, there are 1.8×10^5 search cells. Allowing at most one false alarm over all search cells (on average) puts the desired probability of false alarm at less

than $(1.8\times10^5)^{-1} = 5.6\times10^{-6}$. The value actually chosen was $P_{fa} = 5\times10^{-6}$. The probability of detection was assigned the value $P_d = 0.8$. Equation (12) can then be solved to find DT = 12 dB.

Figure 3 shows curves of $\mathrm{TS_{FOM}}$ as a function of frequency for a range $r = 1$ km. The frequency dependence of the curves results entirely from $J(f)$, and is described by the model for ambient noise and the absorption coefficient in Sec. 2.11.1. The curves in the figure below in fact have the same shape as the curve in Figure 2 corresponding to $r = 1$ km; they are shifted upward or downward according to the other terms in the sonar equation.

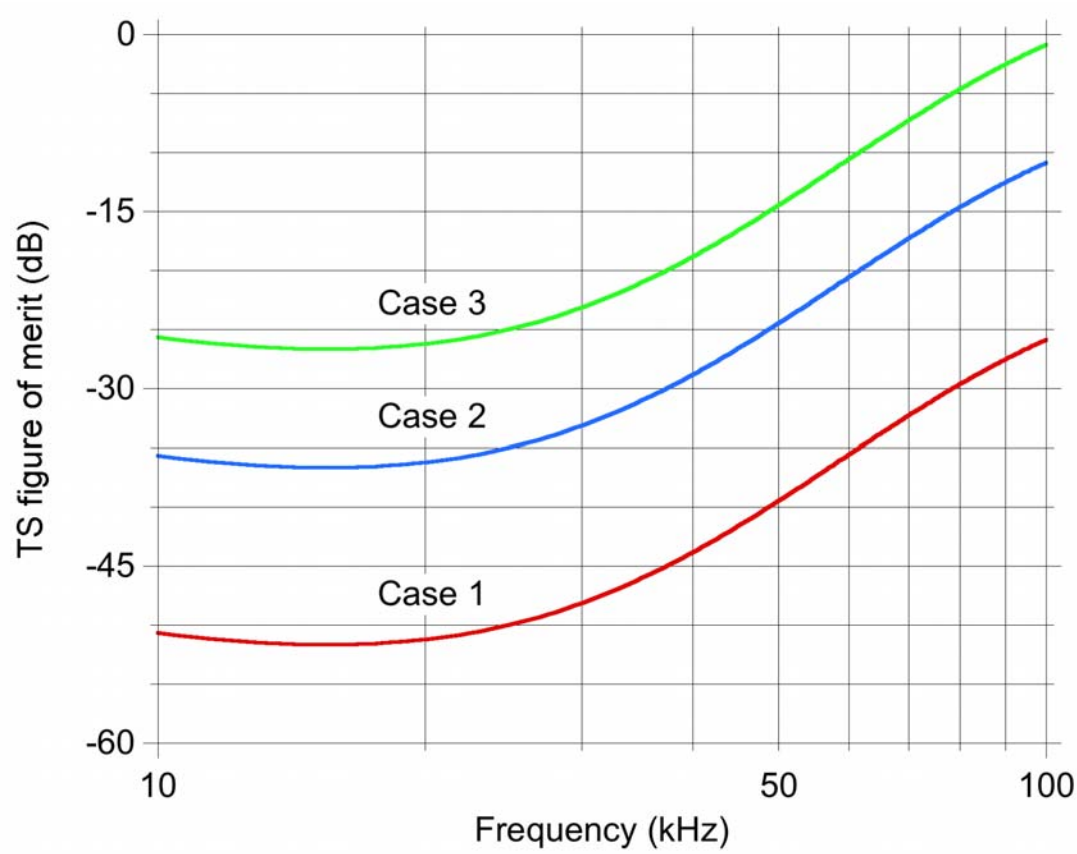

Figure 3: The figure of merit for the target strength for a target at 1 km range. If the actual target strength exceeds the figure of merit, the signal excess is positive. Parameters for the three cases appear in Table 3.

The parameters of Case 1 are clearly favourable for detection. The detrimental effect of absorption loss is evident at the upper frequencies, although the FOM for a target at 1 km range is still only -25 dB at 100 kHz. Under the less favourable conditions of Case 2, however, the need to operate at lower frequencies clearly makes itself felt. At 100 kHz, the FOM for a target at 1 km is now about -11 dB, implying marginal detection of a small mammal at that frequency. Case 3, with a high noise level, of course yields poorer performance.

2.12.2 Example 2: Surface reverberation

In this example, the effect of surface reverberation on detection performance is examined. Although surface reverberation must of course be taken into account when assessing the detection performance against a marine mammal at shallow depth, more generally it will have an effect whenever a reverberant surface area is in the sonar's field of view, regardless of whether the mammal is near the surface or not. For a sonar incapable of steering away from the surface, this example would therefore represent a typical situation. Target motion will not be considered, either because the mammal is loitering in one spot or because the sonar processing is insensitive to Doppler.

Proceeding as in the previous example, the requirement $\mathrm{SE}_R \geq 0$ can be used in conjunction with Eq. (2) to derive a figure of merit for target strength in reverberation-limited conditions:

$$\mathrm{TS}_{\mathrm{FOM}} \equiv \mathrm{S} + 10\log A + \mathrm{DT}. \tag{21}$$

We now select numerical values for the terms on the right-hand side.

The uncertainty in the experimental data for the backscattering strength S was noted earlier in Sec. 2.9.2. It will be assumed that the sonar is hull-mounted and hence located just below the surface; the surface grazing angle will therefore be very low, perhaps less than a few degrees. A graph of scattering strength as a function of wind speed at a grazing angle of 3° appears in [11]. A worst-case value for the backscattering strength can be taken as $\mathrm{S} = -30$ dB, occurring at high wind speeds (greater than 10 m/s, or 20 kt). A value $\mathrm{S} = -50$ is appropriate for a 5-m/s (10-kt) wind speed, and S may drop below -60 dB at very low wind speeds.

The next step is to evaluate the scattering area A defined in Eq. (13). The parameter values that will be used in the calculation are given in the following table:

Table 4: Parameters used for reverberation examples.

$r = 1000$ m
$c = 1500$ m/s
$W = 400$ Hz
$\Theta = 4°$ or 0.07 rad

The parameter values are largely self-explanatory. The bandwidth W is assumed to be 400 Hz, representing either a CW pulse of 2.5-ms duration or a longer-duration FM pulse with a 400-Hz sweep. Substituting the numbers into Eq. (13), we find that the scattering area is $A = 131\,\mathrm{m}^2$, or $10\log A = 21$ dB re 1 m^2.

Lastly, a value DT=12 dB will be used as in the previous example. Equation (21) was now used to compile Table 5, which shows values of $\mathrm{TS}_{\mathrm{FOM}}$ for different assumed values of the scattering strength S. It is concluded that if there is strong surface backscattering, as specified by $\mathrm{S} = -30$ dB, it would be difficult to detect a small mammal such as a dolphin. In calm weather, however, surface reverberation should not prevent the detection of even small marine mammals.

Table 5: Figure of merit for target strength in surface reverberation.

Wind speed (kt)	S (dB)	TS_{FOM} (dB)	Detection performance
> 20	–30	3	Only strong targets
10	–50	–17	Generally good; marginal for dolphins
< 5	–65	–32	Excellent

2.12.3 Example 3: Bottom reverberation

In this example, a marine mammal is close to the ocean bottom and the sonar must cope with reverberation from the seabed. As in the previous example, target motion will be ignored. The water is assumed to be 500 m deep with an isovelocity sound-speed profile, for which the propagation paths are straight lines. The mammal is 10 m above the bottom at a slant range of 1000 m from the sonar. For simplicity in working the numbers, the sonar is assumed to be located at the surface (i.e., the sonar depth is ignored).

The only numerical difference from the previous example will be the value of the backscattering strength, S, which now pertains to the seabed. To extract an appropriate value for S from published experimental data, we need to know the grazing angle at the bottom, and from the problem geometry this is found to be 30º. This angle is large compared to the small grazing angle at the sea surface. Note, however, that in retaining $\Theta = 4°$ as the equivalent azimuthal beamwidth, it must be assumed that the beam pattern has been directed downward and is pointing in the approximate direction of the target. If the beam pattern were pointing horizontally, a target at a 30º depression angle would likely be well outside the mainlobe of the beam. Using values from published data [1],[10] , the following table was assembled:

Table 6: Figure of merit for target strength in bottom reverberation. Range is 1000 m.

Bottom type	S (dB)	TS_{FOM} (dB)	Detection performance
Rock	–10	23	Only very strong targets
Sandy gravel, coarse sand	–25	8	Only strong targets
Fine silt	–40	–7	Marginal

The conclusion is that the target strength of the mammal would have to be large in order to make a reliable detection against bottom reverberation, given the parameters assumed in this example. A fine silt or mud bottom would represent the best case, but even then the FOM of −7 dB would render the detection of dolphins sporadic at best.

If we ask what measures could be taken to obtain additional processing gain in the sonar set to combat seabed reverberation for a stationary target, the only possibility at our disposal is to reduce the reverberation area A, either by increasing the pulse bandwidth W or by decreasing the effective azimuthal beamwidth Θ. For example, increasing the pulse bandwidth to 1000 Hz would result in a theoretical improvement of 4 dB. However, note that the radial width of the reverberation area would be decreased to just $c/2W = 0.75$ m in extent, and the target itself would perhaps be over-resolved, leading to echo-splitting among range bins. As for a possible

reduction in Θ, it should be noted that the effective beamwidth Θ as defined in Eq. (14) will in general be wider than the -3 dB beamwidth. The $\Theta = 4°$ value assumed above may correspond to a -3 dB width of less than 3°, which is approaching the limit of what is found in existing technology.

In the calculations carried out for this example, the fact that the mammal is 10 m above the bottom was never explicitly used. It was nevertheless used implicitly, because it was assumed that the target and the bottom were in such close proximity that they appeared in the same beam; i.e., that they could not be separated by vertical directivity in the beam pattern. An additional calculation indeed shows that the vertical angular separation between the mammal and the reverberation area (both at a slant range of 1000 m) is only 0.7°, and therefore the assumption that they are in the same beam is a good one. This result also supports the assumption made in deriving Eq. (2), namely that the target and reverberant patch are in such close proximity that the transmission loss is the same for both.

Extending these considerations to more general scenarios, it is of interest to examine the effect of vertical directivity in connection with seabed reverberation. In the following two figures, straightline propagation will be assumed, with the sonar located at the surface. Figure 4 shows the maximum depth that would be in the sonar's field of view at a slant range of 1000 m for

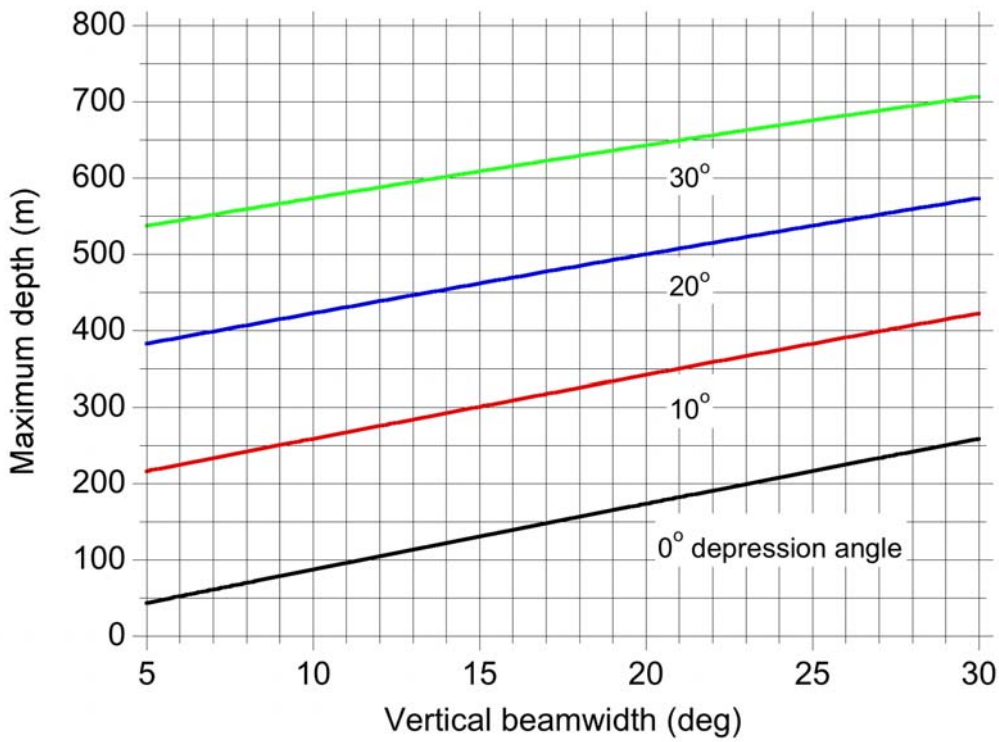

Figure 4: Maximum depth in the sonar's field of view at a slant range of 1000 m for various beam depression angles and vertical beam widths. The sonar is assumed to be at the surface.

various combinations of beam depression angle (i.e., downward steering angle) and vertical beam width. For example, in 100 m of water, bottom reverberation would be received if the beam width exceeded 11° (±5.5° about the MRA) while steering horizontally. Next considered is the vertical angle subtended at the sonar by a target and the seabed for different target depths. Figure 5 shows theoretical curves for three different water depths, with a slant range of 1000 m in all cases. For 200-m deep water, the angular separation is less than 10° except when the target is close to the surface. For 800-m deep water, the angular separation between the target and the seabed is quite large for most target depths, and in this scenario it should be possible to use vertical directivity to avoid bottom reverberation for a mammal located almost anywhere in the water column.

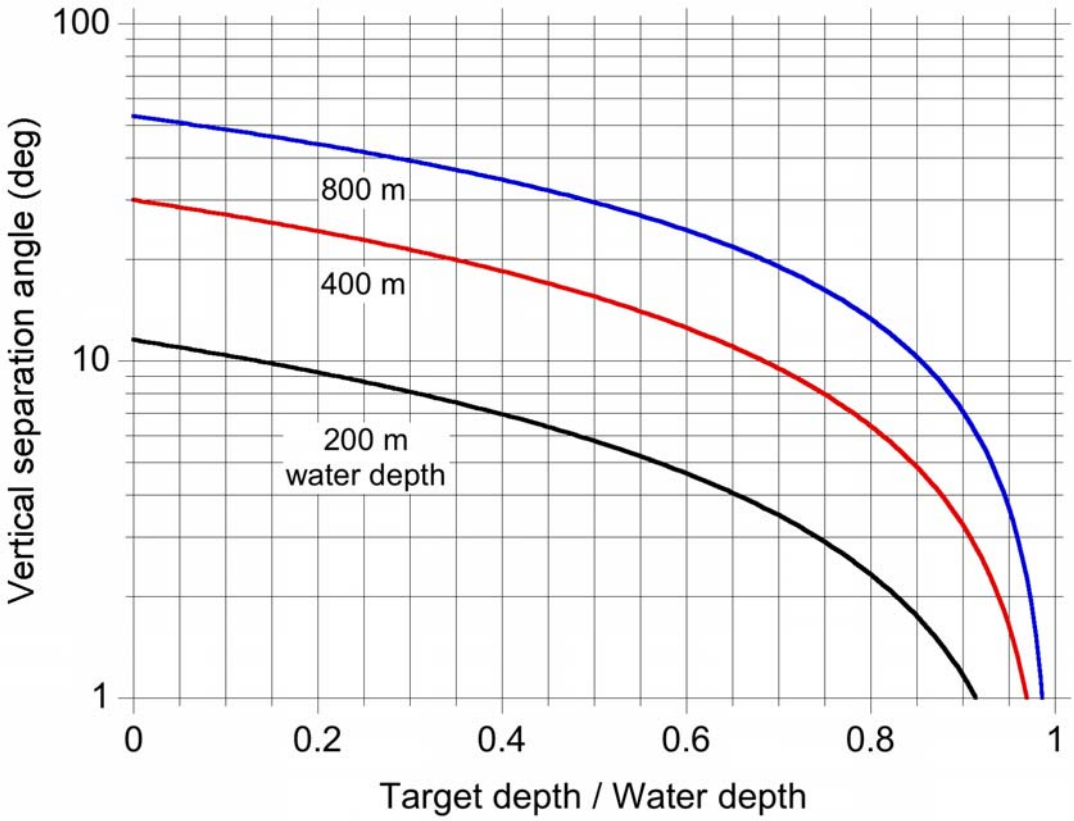

Figure 5: Vertical angle subtended at the sonar by a target and the ocean bottom, both at a slant range of 1000 m. The sonar is located at the ocean surface. The curves correspond to three different water depths.

2.12.4 Example 4: Doppler processing

The above analysis suggests that reverberation, particularly bottom reverberation in shallow water, could potentially degrade the performance of AAM below an acceptable level. There are several measures that could be taken to improve performance by attempting to reduce the reverberant scattering area, as discussed previously. However, in those cases where such

measures are insufficient, Doppler processing becomes a useful approach for combating the interference due to reverberation. In what follows, it will be assumed that a CW pulse is employed, since such pulses are generally the only Doppler-sensitive waveforms available in those commercial sonars having potential application to AAM.

For a narrowband signal, such as the CW signal assumed here, the Doppler effect can be modelled as a simple frequency shift. For a monostatic geometry the shift is given by

$$\Delta f = \frac{2v}{c} f_0, \tag{22}$$

where v is the radial speed of the target relative to the sonar, f_0 is the frequency of the CW pulse, and c is the speed of sound in water. Now, for a CW pulse with a rectangular envelope, the ambiguity function in the Doppler dimension is given at zero range delay by [15]

$$\left|\chi(0,\Delta f)\right|^2 = \mathrm{sinc}^2(\pi \Delta f\, T), \tag{23}$$

where T is the pulse duration and $\mathrm{sinc}(x) = \sin(x)/x$. The normalization is such that the main reverberation peak at zero Doppler ($\Delta f = 0$) has magnitude unity. A target echo with a Doppler shift as given in Eq. (22) sees a reverberation level reduced by approximately ([2], Sec. 15.5.4)

$$20\log(\pi\,|\Delta f\,|T) = 20\log\left(\frac{|\,v\,|\,\omega_0 T}{c}\right), \tag{24}$$

where it has been assumed that the target echo is separated from the zero-Doppler peak, and that the sinc function can be approximated in that region by its $1/x$ envelope. The halfwidth of the zero-Doppler ridge, as measured from its maximum value to the first null of the sinc function in Eq. (23), is given by $T^{-1} = W$. The total scattering term in the sonar equation is given by

$$\mathrm{S} + 10\log\left(\frac{cT}{2}\Theta r\right) - 20\log(\pi\,|\Delta f\,|T). \tag{25}$$

Note that if the pulse length T is increased, the boundary reverberation increases owing to the greater scattering area [the second term in Eq. (25)], but a net reduction in reverberation level still occurs due to the last term in the equation. Thus the principle is much different than for an FM pulse, where wide bandwidth is used to reduce the scattering area.

Let us now revisit the previous example, where bottom reverberation was present and dominant. Assume an operating frequency $f_0 = 40$ kHz, and that the radial target speed is 2 m/s (or about 4 kt). The Doppler shift as calculated from Eq. (22) is $\Delta f = 106.7$ Hz. The target is assumed to be approaching the sonar, so that the Doppler shift is positive, or upwards in frequency. In the parameter set used for computing reverberation (Table 4), the signal bandwidth was assigned a value of $W = 400$ Hz, corresponding to $T = 2.5$ ms for a CW pulse. The halfwidth of the zero-Doppler ridge is also 400 Hz, or almost four times the echo offset $\Delta f = 106.7$ Hz. Therefore the echo would not be separated from the zero-Doppler reverberation, and a longer pulse (narrower bandwidth) is called for. If the pulse duration is increased by a factor of 10 to $T = 25.0$ ms, the width of the zero-Doppler ridge is reduced to 40 Hz, and the echo is now separated from the ridge in the Doppler dimension. The total improvement in signal excess would be about 8 dB: the

scattering area A increases by 10 dB owing to the longer pulse, but the reduction term in Eq. (24) works out to about 18 dB, yielding a net reduction in reverberation level by 8 dB. The results in Table 6 can be adjusted by this amount to produce the following table.

Table 7: Figure of merit for target strength in bottom reverberation with Doppler processing of 4-kt target. Range is 1000 m.

Bottom type	S (dB)	TS_{FOM} (dB)	Detection performance
Rock	–10	15	Only strong targets
Sandy gravel, coarse sand	–25	0	Moderate
Fine silt	–40	–15	Generally good; marginal for dolphins

Although detection performance has of course improved, detection in reverberation from a rocky bottom would still appear to be problematic. However, the signal excess against a fast-moving target (4 m/s, or approximately 8 kt) would be 6 dB better. Finally, it should be pointed out that the gains discussed in this example would be realized only by a sonar set capable of performing the necessary Doppler processing.

2.12.5 Example 5: Shadow zone

One propagation effect that bears on the issue of detection range, particularly when the sonar and target are both close to the surface, is the so-called "shadow zone", an ocean area where the propagation loss is large, perhaps much larger than would be caused by spherical spreading. For example, when the sound-speed profile is downward refracting, there will be a range beyond which there is no direct path (DP) between the sonar and the target. Adequate sonar coverage of that target would have to depend on bottom-reflected rays, but if such rays are greatly attenuated the target is effectively in a shadow zone (see Figure 6). Strong attenuation may occur at the bottom interface, or the transmitter may direct energy away from the bottom.

How a shadow zone could affect the detection of near-surface targets is shown in Figure 7, which is based on a sound-speed profile having a downward-refracting gradient of 0.1 s^{-1}. Two sonar depths are considered, depths that are considered representative for sonars mounted on a ship's hull. For combinations of target depth and range that lie below a given curve, a direct path exists between the sonar and the target; above the curve, the target is not insonified by direct-path energy. In the latter case, the target is in a shadow zone (assuming that no bottom-reflected paths "fill in" the zone). For example, with a sonar at 5-m depth and a target at 7-m depth, a direct path would exist out to a range of about 850 m (red curve), at which point the direct path would be lost. The sonar at 10-m depth would have a direct path to the same target out to a range of 1.0 km (blue curve).

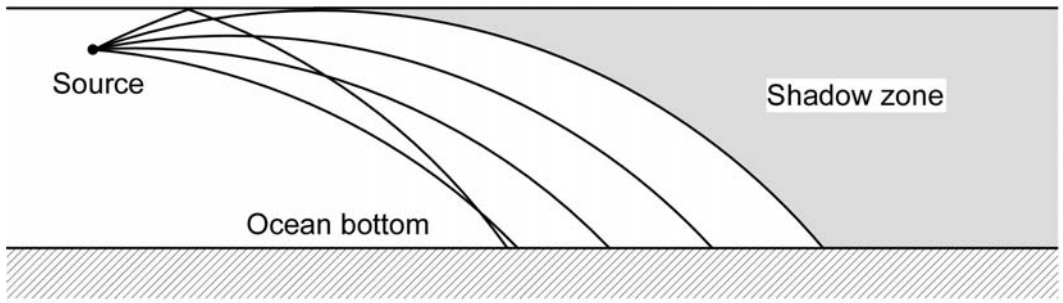

Figure 6: Schematic ray diagram of a shadow zone in a downward-refracting ocean. It is assumed that the sound energy is strongly attenuated by the ocean bottom.

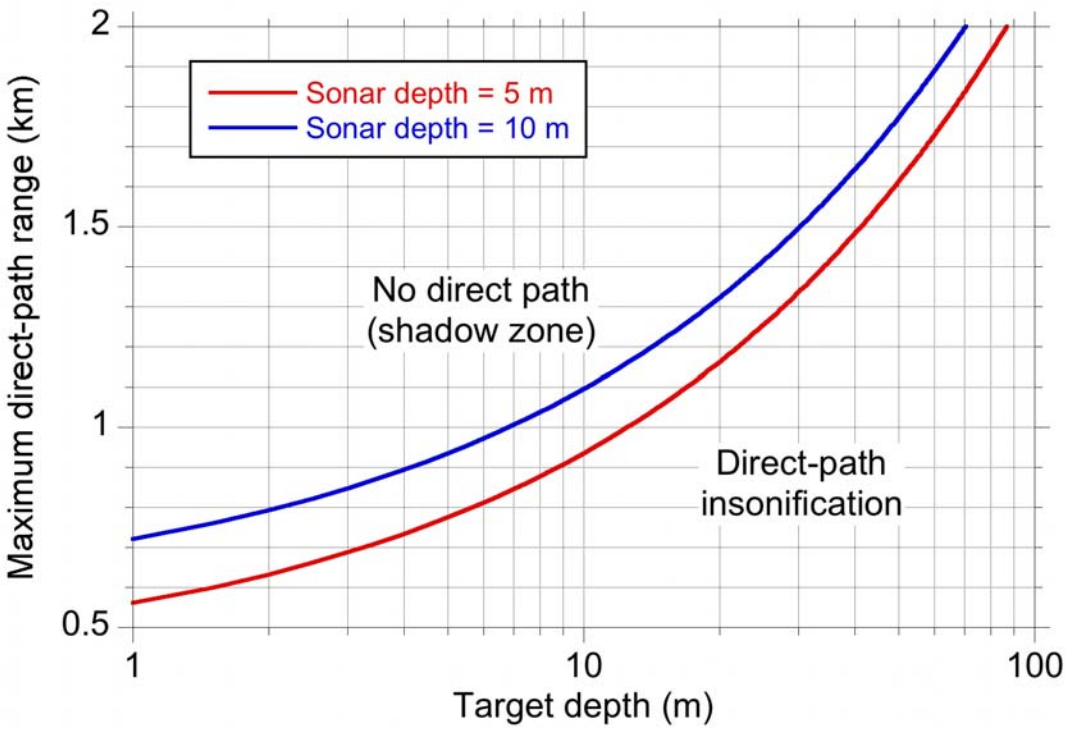

Figure 7: Boundaries of the shadow zone for a downward-refracting gradient of 0.1 per sec.

3 Target Strength

3.1 Target Strength

Target strength (TS) is defined as the ratio, on a decibel scale, of the acoustic intensity (I_s) scattered in a particular direction to the incident acoustic intensity (I_i), or $\mathrm{TS} = 10\log_{10}(I_s/I_i)$, where the scattered and incident intensities are determined at unit distance from the acoustic center of the target. Alternatively, the intensity parameters used in the above formulation may be replaced by expressions for pressure (p) under the plane-wave approximation, $p^2 = \rho c I$, where ρ is the density of the fluid medium and c its sound speed. This leads to the following expression for target strength,

$$\mathrm{TS} = 20\log_{10}\left(\frac{p_s}{p_i}\right) + 20\log_{10}\left(\frac{r}{r_0}\right) \tag{26}$$

where p_s and p_i represent, respectively, the effective scattered and incident acoustic pressure. Note that p_s is measured at a specific location (field point, r) in the far field while p_i is measured at the target location. The second term in the equation corrects to the reference measurement distance (r_0) of one unit of length (usually 1 m) and both r and r_0 are measured with respect to the acoustic center of the target.

There are a variety of primary scattering mechanisms which must be accounted for in target strength modeling. Typically, the most important contribution is specular reflection where an acoustic plane wave from the source "bounces" from a scatterer and travels to the receiver. For *monostatic* target strength (the primary issue here), the measurement field point or sonar receiver position lies in the direction back towards the source location and this is referred to as *backscatter*. For *bistatic* target strength, the measurement point may lie in any direction relative to the target.

3.2 Measured TS

It is very difficult at the best of times to measure TS in the field even for cooperative and comparatively large targets such as submarines. It is even more difficult to do so for marine mammals as controlled conditions are generally not possible. In spite of this, several sets of TS data are available although somewhat limited in completeness or detail. These are shown in references [16] through [20]. These experiments include results for humpback, gray, and sperm whales and a single controlled experiment for a dolphin. There is also little overall sampling with respect to frequency with only the dolphin case examined at a number of frequencies. The results are summarized in the following subsections.

3.2.1 Humpback Whale

Frequency	Whale Size	Aspect	Target Strength
10 kHz	10m	Broadside	2 dB
20 kHz	15m	Broadside	7 dB
20 kHz	15m	Bow	-4 dB

Figure 8: Humpback Whale

3.2.2 Gray Whale

Frequency	Whale Size	Aspect	Target Strength
23 kHz	14m	Stern	3-4 dB
23 kHz	14m	Broadside	8.7 dB

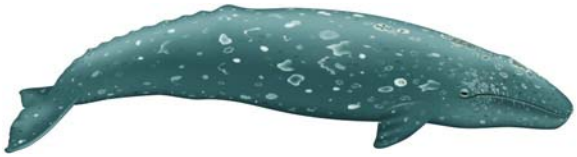

Figure 9: Gray Whale

3.2.3 Sperm Whale

Frequency	Whale Size	Aspect	Target Strength
1 kHz	17-20m est.	Bow ?	-7.2 - -6.0 dB
1 kHz	17-20m est.	Broadside ?	0-10 dB est.

Figure 10: Sperm Whale

3.2.4 Dolphin (Atlantic Bottlenose)

Frequency	Whale Size	Aspect	Target Strength
23-80 kHz	2.2m	Broadside	-10 - -25 dB
67 kHz	2.2m	Pattern	See Ref

Figure 11: Atlantic Bottlenose Dolphin

3.3 Predicting TS

Defence Research and Development Canada (DRDC) has developed boundary element software for predicting the target strength of underwater targets. This AVAST [21][22] software can use either the boundary integral equation method or the Kirchhoff approximation to evaluate the target strength of a complex three-dimensional shape. DRDC has also been involved with the development of a two-dimensional analytically-based software tool for the rapid prediction of target strength. This software, the Bistatic Acoustic Simple Integrated Structure (BASIS) Target Strength Model [23] was jointly developed by researchers at the Naval Research Laboratory (NRL) in the USA, DRDC Atlantic in Canada, and the Defence Science and Technology Organization in Australia. Established methods, including AVAST, for making high-fidelity target strength predictions can be very computationally intensive and involve detailed geometrical models which require significant amounts of time to develop. As a result, operations researchers and naval operators often use a single monostatic target strength value, or a limited number of bistatic values, in their work. BASIS was intended to provide operations researchers with a straightforward way to construct simple but sufficiently accurate models of submarine targets from a handful of simple shapes, using only minimal knowledge of the details of the actual target, and then use reliable analytic approximations to produce fast but reasonably accurate target-strength results in the frequency band from approximately 250 to 2500 Hz.

3.4 BASIS Models

As a very rapid initial analysis, a BASIS model was constructed in an attempt to approximate a whale, in this case the gray and humpback whales. While accuracy was not expected, it was hoped that some understanding could be derived from this quick look.

A 2D BASIS model was constructed using the cylinder, bow ellipsoid, tail cone, and tail sphere primitives. The values used are shown in the table below. The tail sphere is simply used to complete the geometry. Note the bow and cone radius is used to indicate the dimension where the head and tail join the midbody. As the midbody radius is an approximation, it does not necessarily match this other radius (even though it seems the whale is now discontinuous). The tail flukes are assumed to be in plane and, thus, not visible in the 2D model.

Table 8: BASIS Parameters for Whales

Primitive Parameters	10m Humpback	15m Humpback	14m Gray
Cylinder length, L	4.6 m	6.9 m	6.4 m
Tail cone length, T_W	2.8 m	4.2 m	4.1 m
Cylinder radius, R_1	0.9 m	1.35 m	1.4 m
Bow ellipsoid length, L_E	2.6 m	3.9 m	3.5 m
Bow and cone radius, R_E	0.8 m	1.2 m	1.2 m
Conical small radius, R_2	0.1 m	0.15 m	0.3 m

The parameter values are simply approximately scaled from the figures included above based on the estimated lengths of the whales.

The following figure shows the BASIS prediction for the full BASIS models and it is clear there is little correlation to the experimental results.

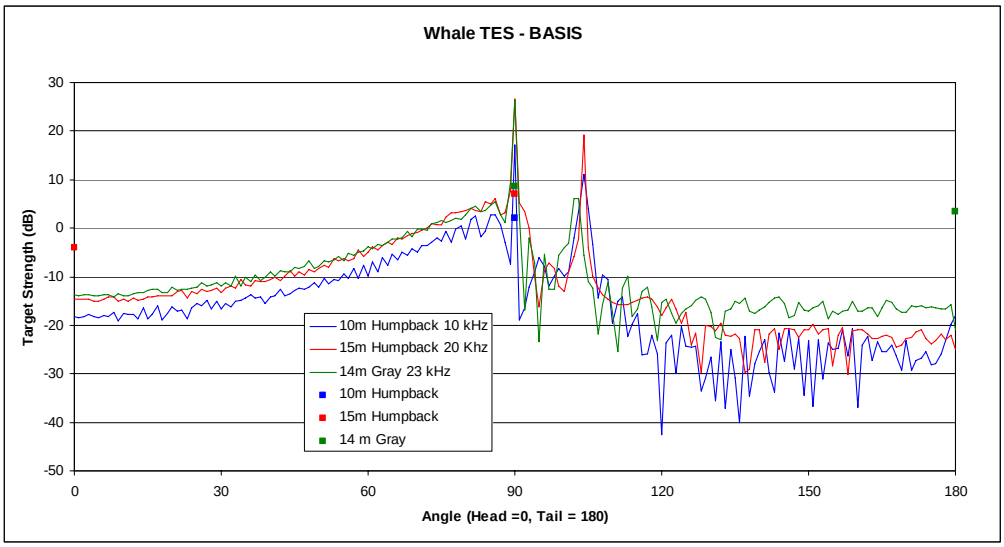

Figure 12: BASIS Results for Whale Target Strength

The broadside values are significantly high than the measured values indicating that the whales cannot, not surprisingly, easily be modeled as perfectly reflecting cylinders. These estimates do match the measured values in a quantitative sense. The value for the 14m gray at 23 kHz and the 15m humpback at 20 kHz are very similar and the variation between the two humpback measurements is approximately 8 dB for the estimate and 5 dB for the measurement. Thus, if the estimates are simply scaled downwards by about 18 dB, then they may have some use for extrapolating to other aspects or whale species.

3.4.1 Whale Lung BASIS Model

As one of the primary reflecting bodies on a whale might be its lung structure, it was attempted to approximate the lungs with a simple BASIS model. Using Figure 7 in Rommel *et al*, the lungs of the whales were modeled on the cetacean presented and scaled in a simple linear fashion. While

this is a very crude approximation, it may provide a bound on the simplicity of the models required. Using this figure, the lungs were modeled as a single ellipsoid of circular cross-section with major dimensions based on the dark shaded profile view of the lungs. The major semi-axis, R_L, and minor semi-axis, R_S, were determined as:

$$R_L = 0.18L/2$$
$$R_S = 0.36R_L$$

where L is the cetacean length. The following table shows the results when using these formulae with our whale examples.

Table 9: Ellipsoid Lung Parameters

Whale	R_L (m)	R_S (m)
10m Humpback	1.8	0.65
15m Humpback	2.7	0.97
14m Gray	2.5	0.91

The BASIS software was used to predict the TS of these ellipsoids and the results are shown in the following figure.

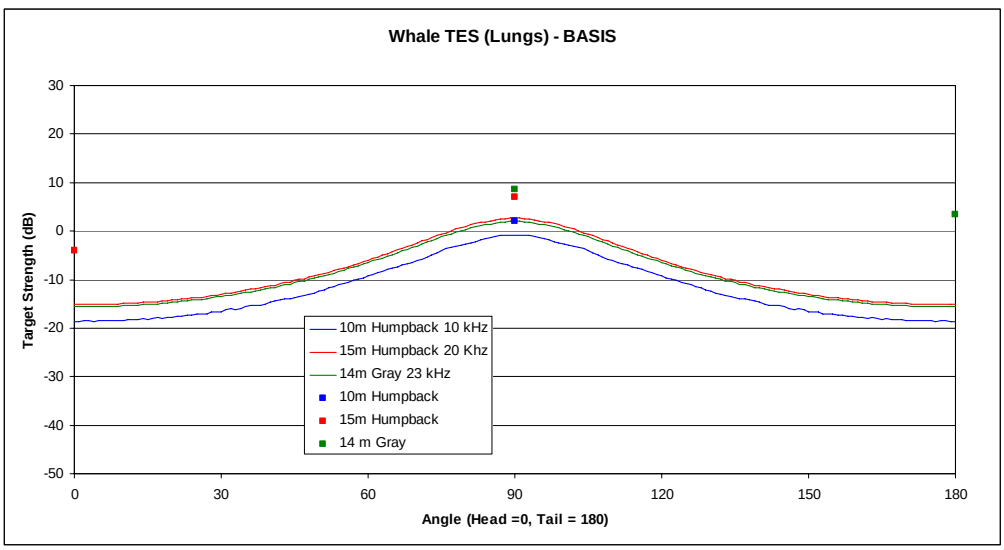

Figure 13: BASIS Model Based on Lungs

Again, while much more accurate on the broadside aspect, the models do not seem to agree well with experiments (under predicting them this time).

3.5 AVAST

As a simple BASIS approximation proved unsatisfactory, it was necessary to create a more accurate and complex detailed model of the whales for use in the AVAST software.

DRDC Atlantic has developed the AVAST software suite for use in the numerical prediction of the acoustic radiation and scattering from floating or submerged elastic structures immersed in infinite, half-space or finite-depth fluid domains. AVAST combines the finite element method for modelling of the structure (if required) with the boundary integral equation technique for representing the fluid. The capabilities of AVAST also include target strength analysis of both elastic and inelastic structures. The boundary integral equation method (BIEM) is one of the available techniques for determining the target strength of a submerged object. Unfortunately, no closed-form solutions exist for arbitrary surfaces. Even for idealized shapes, the number of analytical solutions is very small. Boundary integral formulations have long been recognized as an elegant and computationally economical method of modelling the compressible fluid loading upon a submerged structure. The strength of an integral formulation of the acoustic problem is the reduction of dimensionality; the three-dimensional pressure field is represented by a two-dimensional integral relationship on the surface of the structure. The elegance of the method is the mathematical simplicity of the resulting integral expressions.

AVAST performs this calculation using geometric models provided by the user which have been discretized into paneled meshes. Note that discretization of the structure is required on only that portion which is exposed to the fluid. Further reductions in model size (number of panels) can be achieved by taking advantage of symmetry (for monostatic target strength only). Care should be taken, however, to ensure that the degree of mesh refinement is sufficient to capture the distribution of the acoustic pressure at the upper end of the prescribed frequency range. AVAST analyses have indicated that on the order of 10-12 boundary element panels per acoustic wavelength are required.

The underlying boundary element based algorithms employed by the AVAST solver are best suited for low frequencies (typically up to 1500 Hz for a submarine-sized target). Attempts to model the acoustic response at higher frequencies can quickly overwhelm the memory/disk-space resources of most computers, primarily due the modelling requirement of 10-12 panels per acoustic wavelength. As such, a Kirchhoff-based scattering approximation has been incorporated within the framework of the AVAST code. Discretization of the model into panels is still required, but the memory requirements for this method are much reduced compared to the BIEM with a tradeoff of slightly reduced accuracy for complex shapes.

3.5.1 AVAST Model

As an AVAST model of a whale is a significant project on its own, it was decided to model one of the whales to determine if the experimental data could be approximated. If successful, further models would be evaluated on a case-by-case basis. The 14m gray whale was selected and a geometric model was created. This geometric model was meshed with a variety of panel sizes from 50mm to 20mm depending on the frequency of interest. Note that the 20mm panel size resulted in a model with in excess of 200,000 panels and this model is only valid to about 30 kHz. To reach higher frequencies, smaller panels are required and the increase in the number of panels varies as roughly the square of the decrease in the panel size. Figure 7 shows the 50mm panel size model. Predictions were made using the Kirchhoff approximation in AVAST and a sample of the results is shown in Figure 8 (where 0º is the head and 180º is the tail of the whale). As can be seen, the model provides a reasonable match at broadside, but not at the stern aspect. While only

two frequencies are shown in Figure 8, the results are similar over a range from 10-30 kHz. Thus, over this range, the TS of this whale is generally frequency independent.

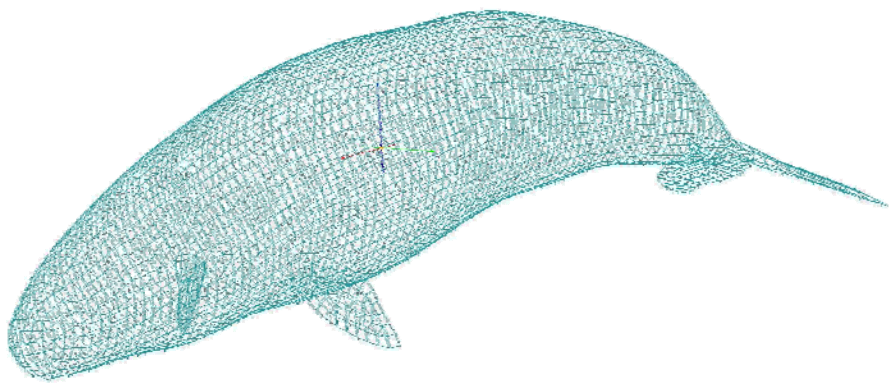

Figure 14: AVAST Gray Whale Model

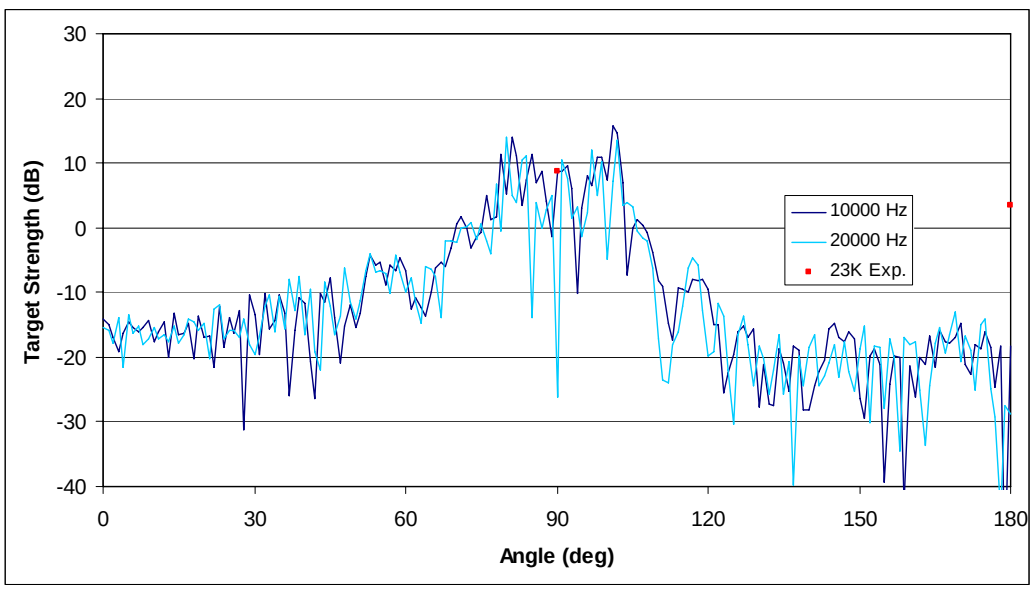

Figure 15: AVAST Gray Whale Target Strength Prediction

For cylindrical models, there are issues with Fresnel zone effects (reference 9) which results in a range variation of TS unless the measurement is made outside of a minimum range (r_{min}) given by $r_{min} > L^2/\lambda$, where L is the length of the cylinder. Using the whale length of 14m, this results in a r_{min} of 2.6 km at 20 kHz. The TS was calculated at a variety of ranges from 250m to 5000m and this effect was not seen. Whether this is due to the lack of a clear cylindrical section of the whale body or the overall streamlined shape is not clear. What seems clear is, that at frequencies up to 30 kHz, the TS is not range dependent.

Given that in biological circles, the TS of fish is often examined and is found to depend heavily on the fish swim bladder, it was theorized that the lungs of the whale might be significant for TS.

As such, a lung model was created and is shown in Figure 16. TS calculations were made and were significantly lower than the overall whale TS at most aspects except the head and tail where the levels approached those of the entire whale model.

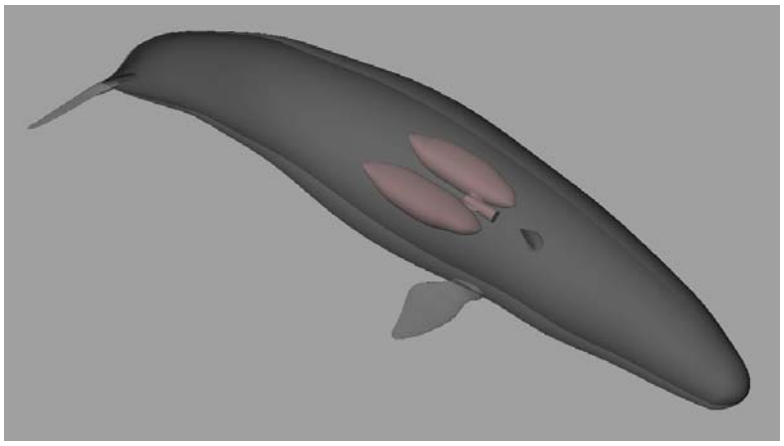

Figure 16: Geometric Gray Whale Model with Lungs

3.5.2 Dolphin TS

After viewing the preliminary results for the 14m whale, it was decided to use this model to estimate the TS for a dolphin-sized target to see if a simple scaling of the model could produce useful results. As such, the 14m whale model was scaled down to 2.2m to match the experimental work done in Reference [20]. In that work, the broadside data ran from about 23 – 80 kHz; however, the directivity was only measured at 67 kHz. When the model was run at two frequencies of 20 kHz and 67 kHz, the results were essentially frequency-independent and matched what was seen with the whale model (not surprisingly, given it is the same model, only smaller). In the reference, the dolphin broadside TS decreases with frequency, unlike what was predicted with AVAST. Also, the model TS drops off faster off broadside than does the data. Thus, the model showed good agreement at broadside at 20 kHz, but not off broadside (assuming the pattern holds across frequency for the data) while the model showed better agreement off broadside at 67 kHz (surprisingly good actually, see Figure 17), but underpredicted the broadside TS. It is not clear how to resolve this. Note that the model also showed no range dependence from 1000m to 7.4m (the measurement range).

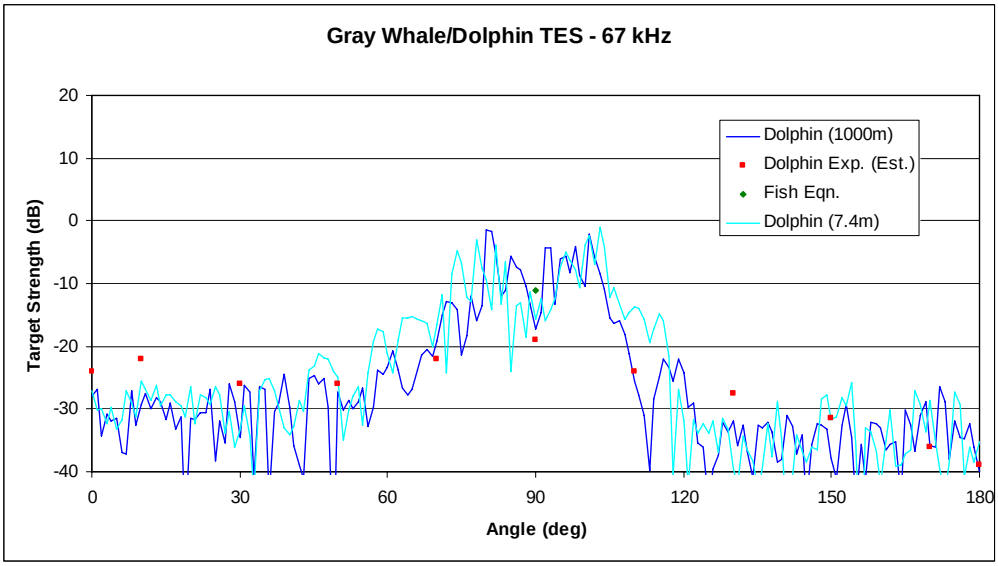

Figure 17: AVAST Dolphin TS Estimate

In Reference [16] (Love) an equation for fish broadside TES is proposed. The following table shows the results of this equation when compared to the measurements and the AVAST predictions. While the results seem accurate, these are only broadside predictions (thus giving no idea as to the directivity) and it is not clear if it holds across frequency for the various whale types. Note that the measured dolphin TS drops with frequency and the equation stays essentially flat.

Table 10: Ellipsoid Lung Parameters

Whale	Frequency	Equation TS	Measured TS
Humpback	10 kHz	3.0 dB	2 dB
Humpback	20 kHz	7.9 dB	7 dB
Gray	23 kHz	7.4 dB	8.7 dB
Sperm	1 kHz	6.3 dB	0-10 dB
Dolphin	23 kHz	-11.0 dB	-11 dB

It is expected at this time that a simple AVAST model will likely yield reasonable TS broadside values as will Love's equation. It is not yet clear what the best solution is to model the directivity although AVAST seems to produce the correct shape of curve.

4 Summary

Under the Exploration and Production (E&P) Sound and Marine Life Programme, a research study was carried out on the feasibility of the Active Acoustic Monitoring (AAM) of marine mammals. The purpose of such monitoring would be to detect marine mammals in those ocean areas where E&P activities are being conducted, in order to allow due diligence in mitigating any potential impact of these E&P operations. The study did not include any direct experimentation.

The AAM study encompassed multiple work components. First, the problem domain was delineated in an overview of offshore E&P activities and of the ocean environments in which they are conducted. To make the analysis more concrete, six specific ocean areas of relevance to E&P were selected and their properties described. Next, the potential performance of AAM was investigated via a parametric study of the sonar equation, incorporating available knowledge of sonar technology and environmental effects (e.g., high-frequency backscattering from the ocean boundaries). This part of the study was intended to identify any fundamental limitations to AAM as imposed by technology or by the basic physics of the problem, and also to pinpoint those sonar features that are of key importance for AAM. Special effort was dedicated to investigating the target strength of marine mammals, as this is an area in which scientific knowledge is sparse at present. The parametric analysis included several generic examples, and was also applied to the six specific ocean areas; however, computer modeling of the six environments was beyond the scope of the study.

This document is one of five Volumes. It provides the technical basis for evaluating the performance of candidate AAM sonars for impact mitigation, concentrating on the range from 500 – 1000 m. It also focuses on the acoustic scattering from marine mammals. Since few data points exist, this report uses submarine target strength models (with validation from the published data points) to investigate the effectiveness of AAM systems and to consider the impact of lung collapse as animals dive to deep water. Some specific results from the analysis are:

- Sound absorption in seawater increases with frequency, and therefore higher sonar frequencies generally result in shorter maximum detection ranges. The most useful sonar frequencies for the AAM problem are below about 50 kHz, while the use of frequencies greater than about 100 kHz would likely not provide long enough detection ranges.

- Classification at long range will be challenging. Typical azimuthal beamwidths will not allow the angular resolution of target structure at such ranges, and the range structure will usually be too ambiguous for classification purposes. This leaves motion as the only reliable clue to classification at long range.

- The sonar should be capable of transmitting and processing both Doppler-sensitive (e.g. CW) and Doppler-insensitive (e.g., HFM) waveforms. The capability of Doppler processing to reject seabed clutter is most important for shallow-water sites.

- At the frequencies of interest for AAM, the ambient noise is largely dependent on the wind speed, although at very high frequencies the thermal-noise component can dominate. In noise-limited conditions, good detection performance can be expected.

- Detection performance in reverberation-limited conditions is more problematic. Surface reverberation alone should not be a problem at low wind speed, but might become important at higher wind speed (high sea state). Detection in bottom-reverberation looks to be difficult in all but the most favorable circumstances, although Doppler processing can help to detect objects that are moving at high enough speed.

- AAM performance is predicted to be good in most deep-water sites, as bottom reverberation is ruled out by the geometry of the detection scenario. Standard values of vertical beamwidth should be sufficient to avoid bottom reverberation out to 1000 m range in water of depth 150 m or even slightly shallower. In very shallow water, however, bottom reverberation would become a factor. AAM performance in shallow water can be predicted with confidence only through the computer modeling of the specific sites of interest.

This page intentionally left blank.

References

[1] R.J. Urick (1983) Principles of Underwater Sound (3rd ed). NY: McGraw-Hill.

[2] W.S. Burdic (1991) Underwater Acoustic System Analysis (2nd ed). Englewood Cliffs, NJ: Prentice-Hall. Reprinted in 2002 by Peninsula Publishing.

[3] R.O. Nielsen (1991) Sonar Signal Processing. Norwood, MA: Artech House.

[4] H. Medwin and C.S. Clay (1998) Fundamentals of Acoustical Oceanography. Boston, MA: Academic Press.

[5] F.B. Jensen, W.A. Kuperman, M.B. Porter, H. Schmidt (2000) Computational Ocean Acoustics. NY: Springer-Verlag.

[6] R.H. Mellen, P.M. Scheifele, and D. Browning (1983) Global Model for Sound Absorption in Sea Water. Technical Report 7923, Naval Underwater Systems Center, 1 October 1983.

[7] R.J. Urick (1984) Ambient Noise in the Sea. Naval Sea Systems Command, Department of the Navy, Washington, DC.

[8] H.L. van Trees (1968) Detection, Estimation, and Modulation Theory, Pt 1. NY: John Wiley.

[9] A.D. Whalen (1971) Detection of Signals in Noise. San Diego, CA: Academic Press.

[10] APL-UW High-Frequency Ocean Environmental Acoustic Models Handbook. Technical Report APL-UW TR 9407, October 1994.

[11] S.T. McDaniel (1993) "Sea surface reverberation: a review." J. Acoust. Soc. Am., vol. 94, pp. 1905–1922.

[12] D.R. Jackson and M.D. Richardson (2007) High-Frequency Seafloor Acoustics. NY: Springer.

[13] J. Simmonds and D. MacLennan (2005) Fisheries Acoustics: Theory and Practice (2nd ed). Oxford: Blackwell Publishing.

[14] I.L. Kalikhman and K.I. Yudanov (2006) Acoustic Fish Reconnaissance. Boca Raton, FL: CRC Press.

[15] C.E. Cook and M. Bernfeld (1967) Radar Signals. NY: Academic Press.

[16] R.H. Love, (1973) Target Strengths of Humpback Whales Megaptera novaeangliae, J. Acoust. Soc. Am., vol. 54, pp. 1312-1315.

[17] Lucifredi, I., Stein, P.J. (2006) Integrated Marine Mammal Monitoring and Protection System (IMAPS): Gray Whale Target Strength Measurements and the Analysis of the Back-Scattered Response, IEEE Oceans 2006 conference.

[18] Miller, J.H., Potter, D.C., Active High Frequency Phased-Array Sonar for Whale Shipstrike Avoidance: Target Strength Measurements, FarSounder White Paper MTS 0-933957-28-9, FarSounder Inc., Warwick, RI.

[19] J.L. Dunn (1969) Airborne Measurements of the Acoustic Characteristics of a Sperm Whale, Letter to J. Acoust. Soc. Am., vol. 46, no. 4 (part 2), pp. 1052-1054.

[20] Au, W.W.L. (1996) Acoustic Reflectivity of a Dolphin, J. Acoust. Soc. Am., vol. 99, 1996, pp. 3844-3848.

[21] Gilroy, L.E., Brennan, D.P. (2000) Predicting Acoustic Target Strength with AVAST, DRDC Technical Memorandum TM 2000-017.

[22] Gilroy, L.E. (2000) Numerically Predicted Aspects of Submarine Target Strength, DRDC Technical Memorandum TM 2000-089.

[23] D.M. Drumheller, M.G. Hazen and L.E. Gilroy (2002) The Bistatic Acoustic Simple Integrated Structure (BASIS) Target Strength Model, Naval Research Laboratory Report NRL/FRMM/7140--02-10019.

Distribution list

Document No.: DRDC Atlantic ECR 2010-044

LIST PART 1: Internal Distribution by Centre

1 Brian Maranda, DRDC Atlantic
1 Layton Gilroy, DRDC Atlantic
1 Jim Theriault, DRDC Atlantic
1 Erin MacNeil, DRDC Atlantic

4 TOTAL LIST PART 1

LIST PART 2: External Distribution by DRDKIM

1 Library and Archives Canada
1 John Campbell, International Association of Oil & Gas Producers (OGP), 209-215 Blackfriars Road, London, SEI 8NL, UK

2 TOTAL LIST PART 2

6 TOTAL COPIES REQUIRED

This page intentionally left blank.

DOCUMENT CONTROL DATA

(Security classification of title, body of abstract and indexing annotation must be entered when the overall document is classified)

1. ORIGINATOR (The name and address of the organization preparing the document. Organizations for whom the document was prepared, e.g. Centre sponsoring a contractor's report, or tasking agency, are entered in section 8.) Defence R&D Canada – Atlantic 9 Grove Street P.O. Box 1012 Dartmouth, Nova Scotia B2Y 3Z7	2. SECURITY CLASSIFICATION (Overall security classification of the document including special warning terms if applicable.) UNCLASSIFIED

3. TITLE (The complete document title as indicated on the title page. Its classification should be indicated by the appropriate abbreviation (S, C or U) in parentheses after the title.)

Survey of Active Acoustic Monitoring (AAM) Technologies: Volume V: Active Sonar Performance Factors

4. AUTHORS (last name, followed by initials – ranks, titles, etc. not to be used)

B. Maranda; L. Gilroy; J. Theriault; E. MacNeil

5. DATE OF PUBLICATION (Month and year of publication of document.)	6a. NO. OF PAGES (Total containing information, including Annexes, Appendices, etc.)	6b. NO. OF REFS (Total cited in document.)
March 2010	58	0

7. DESCRIPTIVE NOTES (The category of the document, e.g. technical report, technical note or memorandum. If appropriate, enter the type of report, e.g. interim, progress, summary, annual or final. Give the inclusive dates when a specific reporting period is covered.)

External Client Report

8. SPONSORING ACTIVITY (The name of the department project office or laboratory sponsoring the research and development – include address.)

International Association of Oil and Gas Producers (OGP)
Joint Oil and Gas Industry Programme on Sound and Marine Life (JIP 22)

9a. PROJECT OR GRANT NO. (If appropriate, the applicable research and development project or grant number under which the document was written. Please specify whether project or grant.) RFP JIP08-05	9b. CONTRACT NO. (If appropriate, the applicable number under which the document was written.) JIP22 08-05
10a. ORIGINATOR'S DOCUMENT NUMBER (The official document number by which the document is identified by the originating activity. This number must be unique to this document.) DRDC Atlantic ECR 2010-044	10b. OTHER DOCUMENT NO(s). (Any other numbers which may be assigned this document either by the originator or by the sponsor.)

11. DOCUMENT AVAILABILITY (Any limitations on further dissemination of the document, other than those imposed by security classification.)

12. DOCUMENT ANNOUNCEMENT (Any limitation to the bibliographic announcement of this document. This will normally correspond to the Document Availability (11). However, where further distribution (beyond the audience specified in (11) is possible, a wider announcement audience may be selected.))

13. ABSTRACT (A brief and factual summary of the document. It may also appear elsewhere in the body of the document itself. It is highly desirable that the abstract of classified documents be unclassified. Each paragraph of the abstract shall begin with an indication of the security classification of the information in the paragraph (unless the document itself is unclassified) represented as (S), (C), (R), or (U). It is not necessary to include here abstracts in both official languages unless the text is bilingual.)

Under the Exploration and Production (E&P) Sound and Marine Life Programme, a research study was carried out on the feasibility of the Active Acoustic Monitoring (AAM) of marine mammals. The purpose of such monitoring would be to detect marine mammals in those ocean areas where E&P activities are being conducted, in order to allow due diligence in mitigating any potential impact of these E&P operations. The study did not include any direct experimentation.

The AAM study encompassed multiple work components. First, the problem domain was delineated in an overview of offshore E&P activities and of the ocean environments in which they are conducted. To make the analysis more concrete, six specific ocean areas of relevance to E&P were selected and their properties described. Next, the potential performance of AAM was investigated via a parametric study of the sonar equation, incorporating available knowledge of sonar technology and environmental effects (e.g., high-frequency backscattering from the ocean boundaries). This part of the study was intended to identify any fundamental limitations to AAM as imposed by technology or by the basic physics of the problem, and also to pinpoint those sonar features that are of key importance for AAM. Special effort was dedicated to investigating the target strength of marine mammals, as this is an area in which scientific knowledge is sparse at present. The parametric analysis included several generic examples, and was also applied to the six specific ocean areas; however, computer modeling of the six environments was beyond the scope of the study.

This report (Volume V) reviews the factors impacting the performance of an AAM system. The basis of discussion is the sonar equation, with particular attention paid to the scattering properties of marine mammals.

14. KEYWORDS, DESCRIPTORS or IDENTIFIERS (Technically meaningful terms or short phrases that characterize a document and could be helpful in cataloguing the document. They should be selected so that no security classification is required. Identifiers, such as equipment model designation, trade name, military project code name, geographic location may also be included. If possible keywords should be selected from a published thesaurus, e.g. Thesaurus of Engineering and Scientific Terms (TEST) and that thesaurus identified. If it is not possible to select indexing terms which are Unclassified, the classification of each should be indicated as with the title.)

Oil and Gas Industry; Active Acoustic Monitoring; Marine Mammals; Marine Mammal Monitoring; Active Sonar;